

# **IN-SITU BIORESTORATION OF NITRATE CONTAMINATED WATER WELLS**

A Report to the  
**Texas Water Development Board**

Prepared by

W. MICHAEL STALLARD  
K. C. WU  
N. SHI  
M. YAVUZ CORAPCIOGLU

DEPARTMENT OF CIVIL ENGINEERING  
TEXAS A & M UNIVERSITY  
COLLEGE STATION, TX 77843-3136

28 February 1994  
Amended 24 June 1994



# **IN-SITU BIORESTORATION OF NITRATE CONTAMINATED WATER WELLS**

A Report to the

**Texas Water Development Board**

Prepared by

W. MICHAEL STALLARD  
K. C. WU  
N. SHI  
M. YAVUZ CORAPCIOGLU

DEPARTMENT OF CIVIL ENGINEERING  
TEXAS A & M UNIVERSITY  
COLLEGE STATION, TX 77843-3136

28 February 1994  
Amended 24 June 1994

## TABLE OF CONTENTS

Summary .....	1
Acknowledgments.....	1
Introduction .....	2
Experimental Studies.....	5
Preliminary Hydraulic Experiments.....	5
Large Tank Experimental Setup .....	7
Experimental Results.....	10
Well without ambient horizontal ground water flow .....	11
Well with ambient horizontal ground water flow.....	15
Ambient horizontal flow, depth distributed pollutant .....	18
Ambient horizontal flow, surface pollutant.....	20
Experiment reproducibility and sensitivity .....	25
Numerical Model .....	28
Model Development.....	28
Solution Technique.....	30
Parameter Estimation and Calibration.....	31
Numerical Results.....	32
Conclusions .....	35
Actions for the Coming Year.....	37
References.....	39
Appendix A–Numerical Modeling Results .....	41

## **SUMMARY**

The first annual report of experimental investigations of a technique for remediating and protecting ground water and drinking water wells from contamination is presented. A ground water remediation well design is proposed in which ground water is drawn into the well bottom, treated in the well casing, and returned clean to the aquifer at the well top. The hydraulics of ground water circulation around perfectly and imperfectly penetrating wells were examined experimentally in pilot-scale tanks and mathematically with two- and three-dimensional computer models. Ambient ground water velocities of from 1 to 3 m/day, typical for coarse sand and gravel aquifers, were simulated in combination with in-well vertical velocities of from 2 m/day to 16 m/day. Under some of these flow conditions, contaminants were intercepted and drawn into the wells for treatment. Hydraulic problems identified with the experimental apparatus and simulated by the computer models included blow-through of contaminant at the well intake by high ambient ground water velocities and submergence by the well hydraulics of surface contaminant plumes without interception. Both types of problems were corrected by adjusting internal well velocities. Important design parameters include ambient ground water velocity and well pumping rate. This study has demonstrated that recirculating ground water remediation wells may be a feasible process for protecting drinking water wells from ground water contamination in a sandy unconfined aquifer.

## **ACKNOWLEDGMENTS**

This project was partially funded by Texas Water Development Board. Their support and advice is gratefully acknowledged. In particular, we would like to thank Phil Nordstrom for his patience and effort. The mention of product names and manufacturers in this report does not constitute endorsement of those products.

## INTRODUCTION

Prevention and remediation of ground water contamination is an important public health concern. Approximately 50 percent of the population of the United States depends on ground water for its primary potable water supply. There is a need for reliable and economical methods of preventing and cleaning ground water contamination.

The reported research involves the development of a recirculating ground water remediation well (RGRW) system to remove contaminants from ground water. The system consists of one or more recirculating treatment wells in which a chemical or biological treatment process is maintained. Contaminated water is drawn from the aquifer into the bottoms of the treatment wells, treated in the wells, and returned to the aquifer near the tops of the wells. The well configuration and recirculation pattern are illustrated in Figure 1.

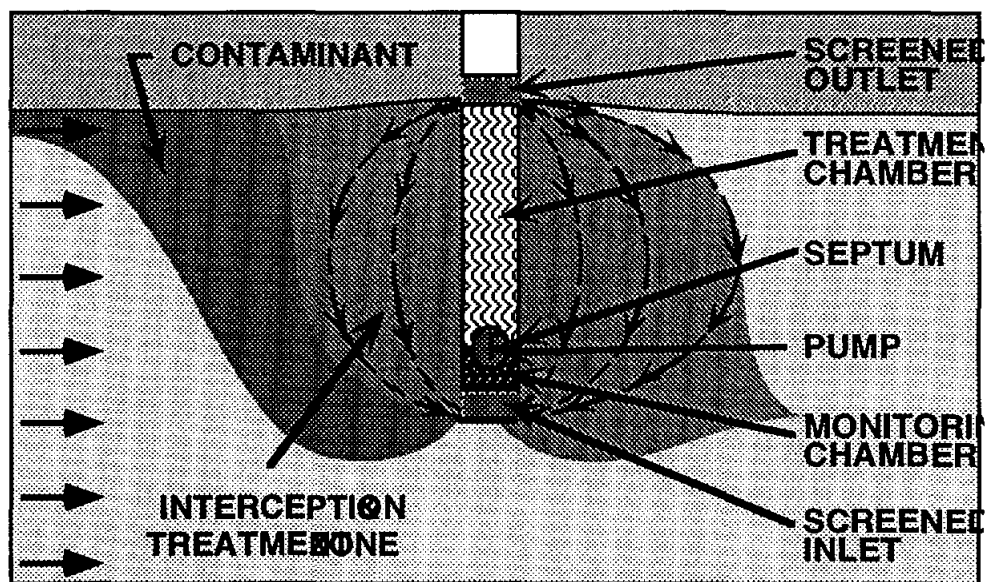
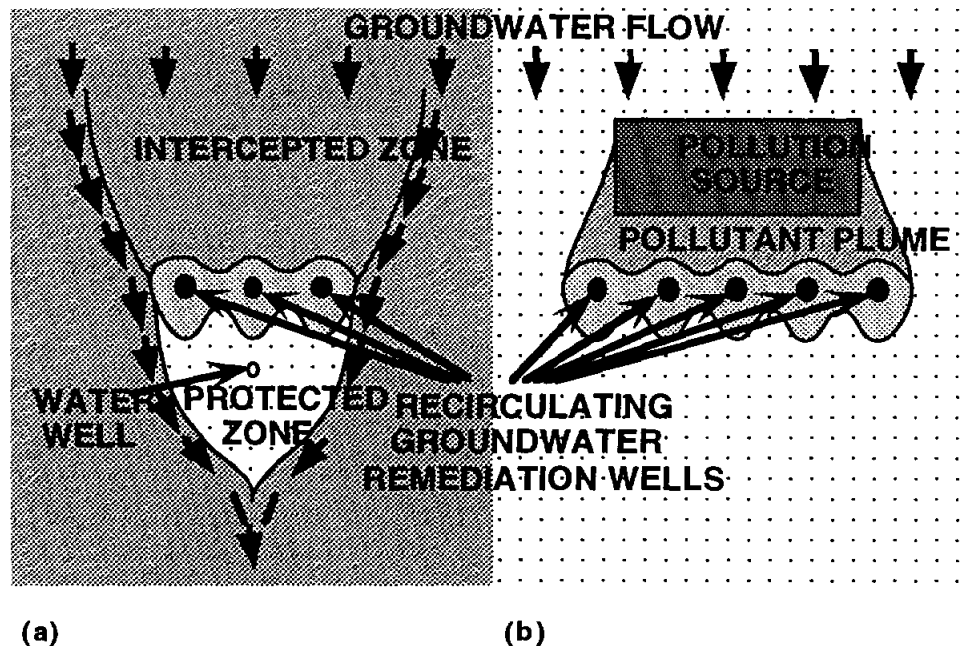


FIGURE 1. Schematic of recirculating ground water remediation well system.

Potential applications for the RGRW system include protection or recovery of wells from contamination by widespread pollutants such as nitrate, and containment and treatment of localized ground water contamination from facilities such as cattle feed lots or from sanitary and secure landfills. The most widespread ground water pollutant in the world today is nitrate, from natural as well as agricultural, industrial, and domestic sources [Spalding and Exner, 1993]. As much as 4 percent of the domestic ground water supply is lost annually to nitrate contamination, compared to less than 0.5 percent of the supply lost to organic

chemical contamination [Spalding and Exner, 1993]. High nitrate concentration in drinking water has been linked to methemoglobinemia (blue baby syndrome), a potentially fatal disease of infants. The United States Environmental Protection Agency (USEPA) has established a drinking water standard of 10 mg/L nitrate as nitrogen.

The RGRW system might be used to restore drinking water wells that are nitrate contaminated or to provide treatment barriers to protect wells threatened by nitrate contamination. The zones of capture of the treatment wells would enclose the protected drinking water well, so that very little untreated water could reach the drinking water well, as illustrated in Figure 2.



**FIGURE 2.** Conceptual recirculating ground water remediation well system applications: a) protection of drinking water well within pollution plume; and b) containment of locally distributed pollution source.

Also shown in Figure 2 is a conceptualization of the use of an RGRW system to contain and treat contaminants from a localized non-point discharge. Many facilities may leak pollutants to ground water over a localized non-point area. These pollutants may include nitrates, organic material, and agricultural chemicals from installations such as feed lots, process and hazardous chemicals from industrial installations such as containment ponds, and leachate from environmental control installations such as landfills.

Pollutants from localized non-point sources might be contained and treated by overlapping zones of capture from RGRWs located along the downgradient side of the facility, as shown in Figure 2. The design and operations of the RGRW system would determine the combination of treated and untreated water that escapes the facility through and beneath the well field.

An important consideration in the development of the RGRW system is the hydraulics of a recirculating well operating in a ground water aquifer. The purpose of this paper is to present results of hydraulic studies of pilot scale model aquifers and to compare those results to numerical models of the RGRW system hydraulics for imperfectly penetrating wells; i. e., for wells that extend only partially through the aquifer.

Hydraulically, the wells are similar to vacuum vaporizer wells used in Germany [Herling and Buermann, 1990] and in-situ stripping wells used in the United States [Coyle, et al., 1988] to remove volatile organic compounds from ground water. These well types have been modeled for perfectly penetrating conditions [Herling and Buermann, 1990; MacDonald and Kitanidas, 1993]. Perfectly penetrating wells are appropriate for a limited number of applications. Many aquifers are too deep for full penetration by a well to be practical. Another disadvantage of perfectly penetrating wells is their tendency to mix a contaminant throughout the aquifer depth. A contaminant such as nitrate may be restricted to the near surface region of the aquifer. Mixing by a perfectly penetrating well would spread the contaminant through the depth and might make it more difficult to remove.

## EXPERIMENTAL STUDIES

A series of tracer experiments were conducted in two ground water simulation tanks to characterize the hydraulic behavior of perfectly and imperfectly penetrating wells. Results of the experiments were used to identify potential problems with the well operation and to calibrate a numerical model, described later in this report. Experiments were conducted without and with a horizontal ambient ground water flow. Different well configurations, internal well velocities, and contaminant/treatment combinations were simulated. The experimental apparatus and results are described in the following sections.

### PRELIMINARY HYDRAULIC EXPERIMENTS

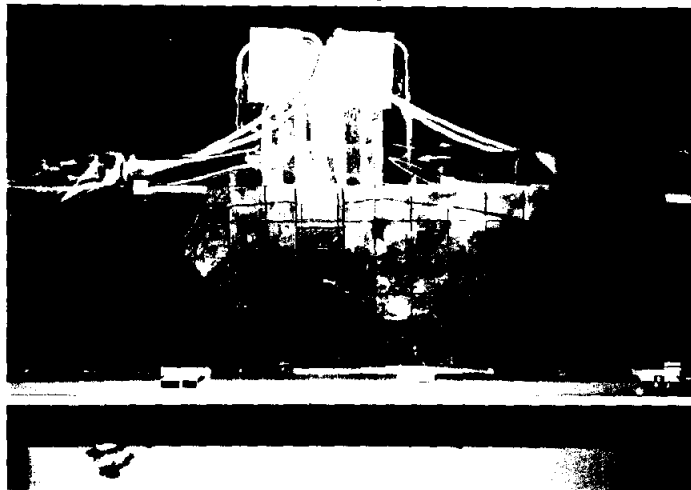
Several preliminary experiments on the hydraulics of the well system were run in a small, relatively shallow tank, shown in Figure 3. For these experiments, a 0.45 to 0.55 mm diameter sand was placed in the small tank. A well, shown in Figure 4, consisting of a section of PVC pipe split longitudinally, was affixed to the side of the tank. The well had slot sections near its upper and lower ends, and completely penetrated the sand bed.



Figure 3. Small ground water tank apparatus.

The tank was filled with the sand and water containing phenolphthalein, a pH sensitive indicator solution. The indicator turned from clear to red when the pH exceeded 8.3. Water was circulated through the well, and the pH in the well was continuously adjusted to pH 12 by the addition of sodium hydroxide solution. As the pollutant (sodium hydroxide) moved through the sand under the influence of the well, the color of the water-sand-

indicator shifted to red. The movement of the pollutant, and therefore the recirculation water flow through the tank, was visible through the tank side, as shown in Figure 4.



**Figure 4. Typical results shown on small ground water tank of hydraulic tests.**

A two-dimensional finite difference computer model of the small tank flow system was developed and calibrated to the small tank data to aid design of a larger scale experimental tank. The model was adjusted to fit the data collected in the preliminary hydraulic experiments. Typical results of the calibrated model are shown in Figure 5 for the pollutant front at different times after the pollutant feed was begun. The water table surface is shown in the figure near the top of the tank. Collected data, taken from the traced pollutant migration fronts, are shown as x's on the plots. All of the preliminary experiments and the modeling were conducted for ground water without horizontal flow. Agreement between the modeled and actual pollutant fronts was very good for the perfectly penetrating well conditions of the experiments.

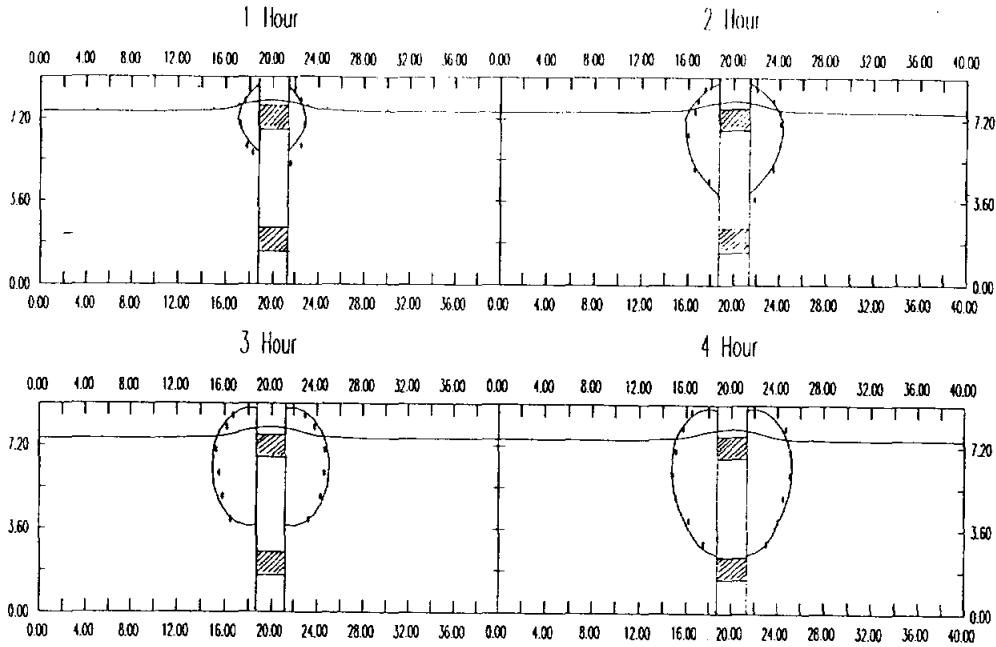


**Figure 5. Comparison of typical modeled pollutant front migration with measured results for small ground water tank apparatus.**

### **LARGE TANK EXPERIMENTAL SETUP**

The experimental apparatus for the second series of laboratory studies consists of a ground water tank, scaled remediation wells, and contaminant monitoring and treatment control system. The design and dimensions of the ground water simulation tank are shown in Figure 6. The tank consists of a stainless steel U-channel frame, reinforced with structural steel, with acrylic sides. The tank is fitted with a series of twelve manometers, so that the piezometric head can be measured at various locations within the tank during operation. In addition, access ports are provided at 10 cm intervals on both sides and the bottom of the tank frame. Water can be introduced or withdrawn, samples can be collected, or head conditions can be monitored at each of these ports. Three-cm diameter vertical tubes extend through the full tank depth at either end of the tank. Each tube has a screened slit along its full length. An ambient ground water flow can be simulated in the tank by introducing water into the tube at one end of the tank, and withdrawing water from the tube at the opposite end.

The tank is filled with a uniform silica sand, of grain size between 0.45 and 0.55 millimeters from Vulcan Materials Co. of Fort Worth, TX. The properties of the sand as placed in the tank are summarized in Table 1. Vertical and horizontal hydraulic conductivities were measured by falling head permeameter tests on samples collected from the tank.

**TABLE 1. Measured properties of model aquifer materials**

Property	Units	Value
vertical hydraulic conductivity ( $K_v$ )	cm/min	7.61
horizontal hydraulic conductivity ( $K_h$ )	cm/min	9.39
porosity ( $n$ )		0.44
bulk density ( $\rho_b$ )	g/cm <sup>3</sup>	2.59

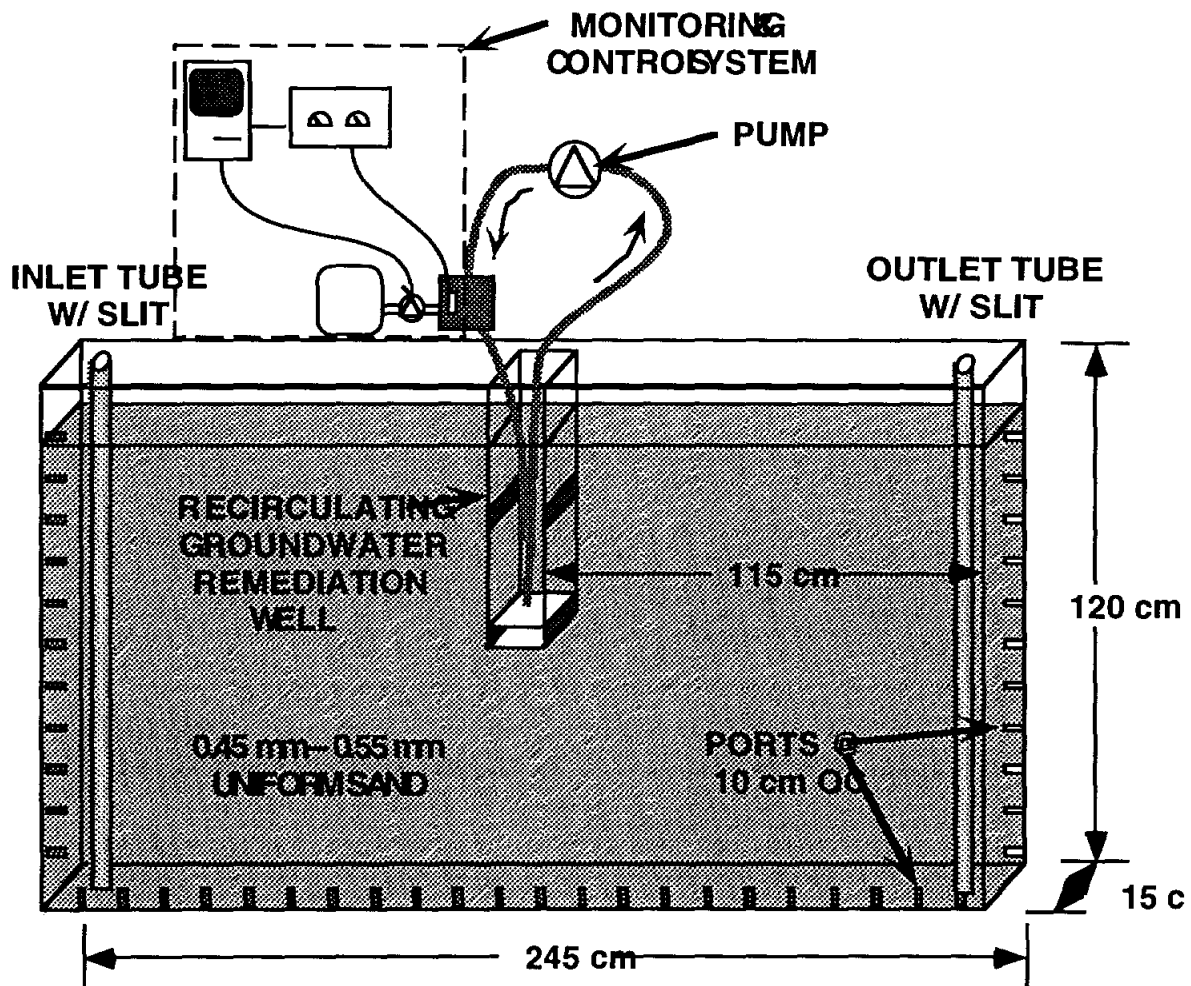


**FIGURE 6. Sketch of ground water tank showing layout and dimensions.**

Two scaled ground water remediation wells, illustrated in Figure 7, were used in the experiments. Each well consists of an acrylic casing, 15 cm long by 12 cm wide. The first well was 60 cm high, and the second well was 50 cm high. The casing of each well is

capped by an acrylic plate at the well bottom. A separation plate, located 5 cm above the well bottom, divides the ground water remediation well into withdrawal and treatment compartments. The sidewalls of the recirculating well withdrawal compartment normal to the tank ambient flow are open, but screened with #200 nylon mesh from Gilson Company, Inc. of Worthington, OH. Similar screened sections 12 cm by 5 cm high are located 20 cm above the separation plate in the treatment compartment in the first well, and 10 cm above the separation plate in the second well.

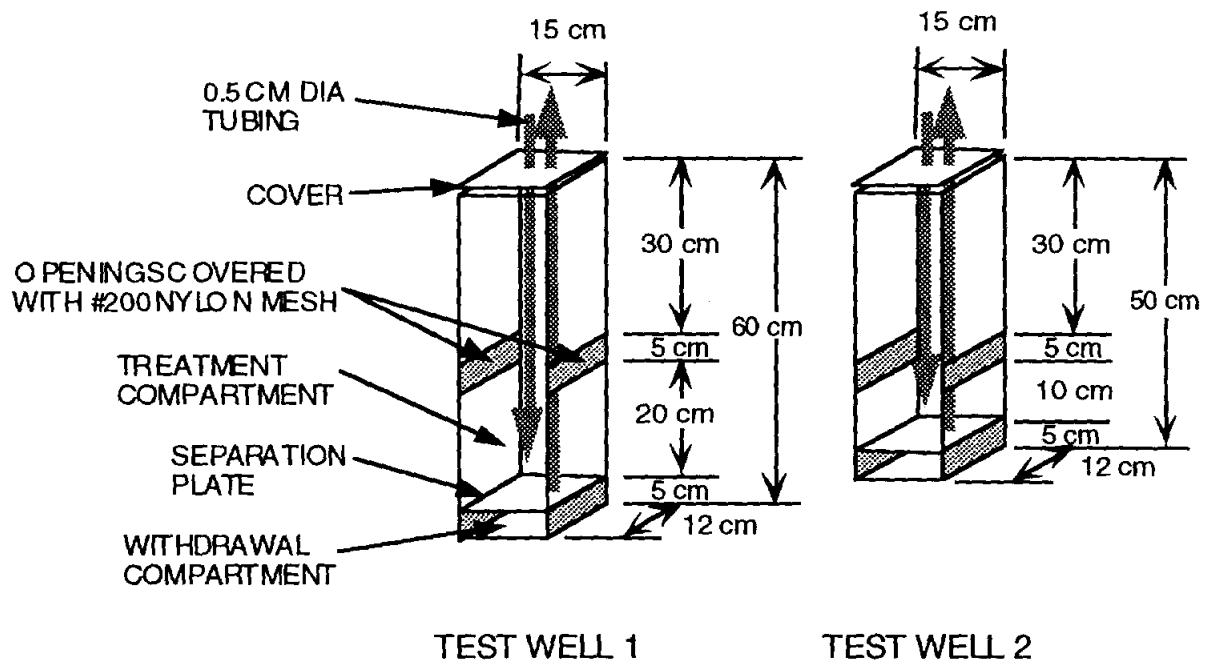


**FIGURE 7. Sketch of scaled recirculating ground water remediation wells 1 and 2.**

The well separation plate is pierced by a 0.5 cm diameter Tygon tube through which water is withdrawn into a peristaltic pump. The pump discharges into a reservoir in which chemical concentrations in the extracted water can be monitored. Chemicals may be added to the reservoir, after which the water is returned to the treatment compartment of the recirculating well. Computer controlled feed mechanisms are provided to add chemicals or nutrients to the monitoring compartment of the well to remove or compensate for ground water contaminants.

The remediation well may be placed anywhere along the tank. The well placement for these experiments is illustrated in Figure 6. The well is located at the longitudinal center, along

one wall of the tank . The recirculating well is 12 cm wide, compared to the 15 cm width of the tank. It does not extend the full width of the tank so that passing flow is allowed, and the well does not behave as a dam in the tank.

A schematic of the monitoring and chemical feed control system is shown in Figure 8. The system consists of an 80486 based desktop computer with data acquisition and terminal cards installed, control software, a pH/millivolt meter, specific ion probe, and computer controlled chemical feed unit. Manufacturers and model numbers for each of the units are shown in Figure 8.

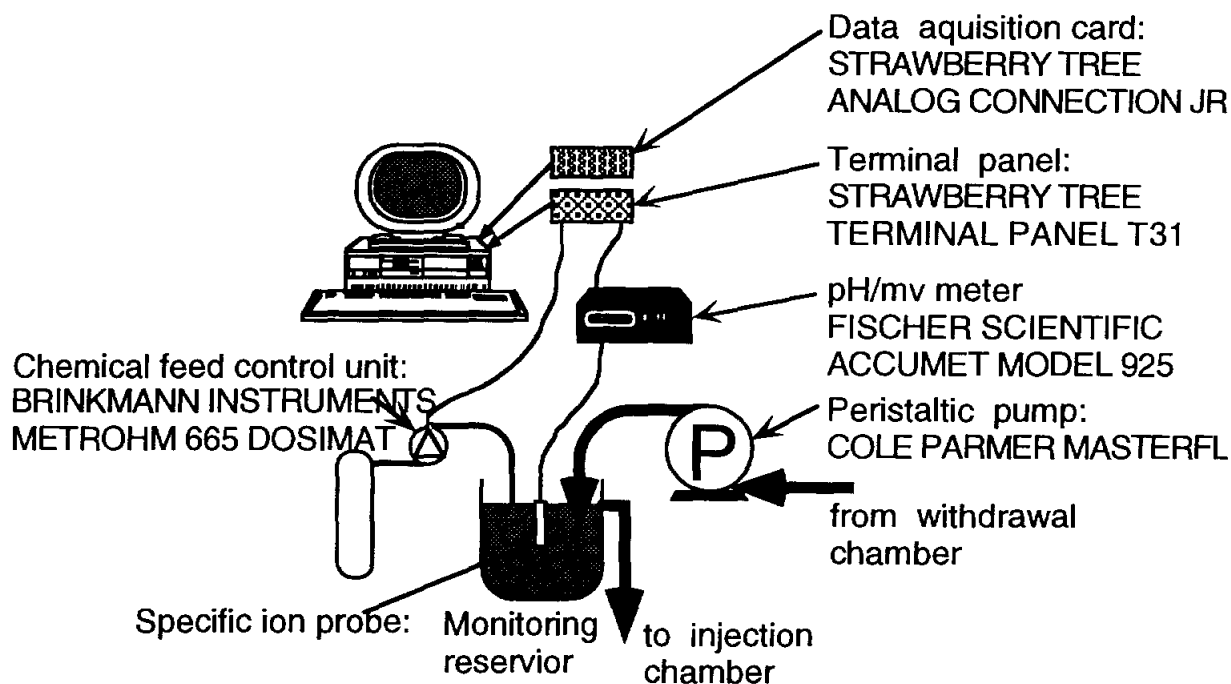


**Figure 8. Schematic of well monitoring and chemical feed control system.**

## **EXPERIMENTAL RESULTS**

Tracer studies were conducted to characterize the hydraulics within the scaled RGRW and surrounding ground water. Water containing phenolphthalein indicator solution and either hydrochloric acid (HCl) or sodium hydroxide (NaOH) was added to the tank. The pH of the water entering the recirculation well was monitored and adjusted. For studies in which the tank water contained HCl, the pH was adjusted to approximately pH 12 by addition of concentrated NaOH solution to the well injection compartment. When the tank water

contained NaOH, HCl was added to lower the pH to 7. The indicator solution remained colorless when the pore water in the tank was less than pH 8.3, but became red when the pH rose above 8.3. The extent of a plume from the well could be monitored visually through the Plexiglas sides of the tank. Results of these experimental studies are presented below.

### **Well without ambient horizontal ground water flow**

The first set of tracer studies was conducted with no ambient horizontal flow in the tank. Water in the tank contained HCl and phenolphthalein. Strong NaOH solution was added to the well with an equivalent volume of water withdrawn, so that the water volume in the tank remained constant. The extent of the plume was monitored over time for different velocities in the RGRW to determine the effects of pumping rate on the development of the NaOH plume. A summary of the tested conditions is given in Table 2.

**TABLE 2. Summary of tested conditions with no ambient flow; NaOH added to recirculating well.**

Well Type	Ambient ground water velocity	Vertical well velocity <sup>1</sup>
1	–	2.0 m/d
1	–	4.0 m/d
1	–	8.0 m/d
2	–	8.0 m/d
2	–	16.0 m/d

<sup>1</sup>Vertical well velocity is defined as the flow rate through the well divided by the well cross-sectional area..

Plume developments for each of the test conditions described in Table 2 are illustrated in Figures 9 through 14. In each case, the plumes developed essentially symmetrically about the well, with a larger plume diameter with greater well pumping rate at a given time in the experiments.

Herling and Stamm [1992] have suggested that the diameter of the plume surrounding a perfectly penetrating recirculating well at hydraulic equilibrium is determined principally by the hydraulic conductivities of the aquifer material, and is independent of the recirculating well pumping rate. The wells in these experiments were not operated to hydraulic

equilibrium because of limitations of the tank size and the time required to approach equilibrium. In these experiments, the plume developed more quickly with higher well pumping rates. The plume diameters, measured as the maximum horizontal distance across the plume, after 24 hours of continuous well operation are shown in Table 3.

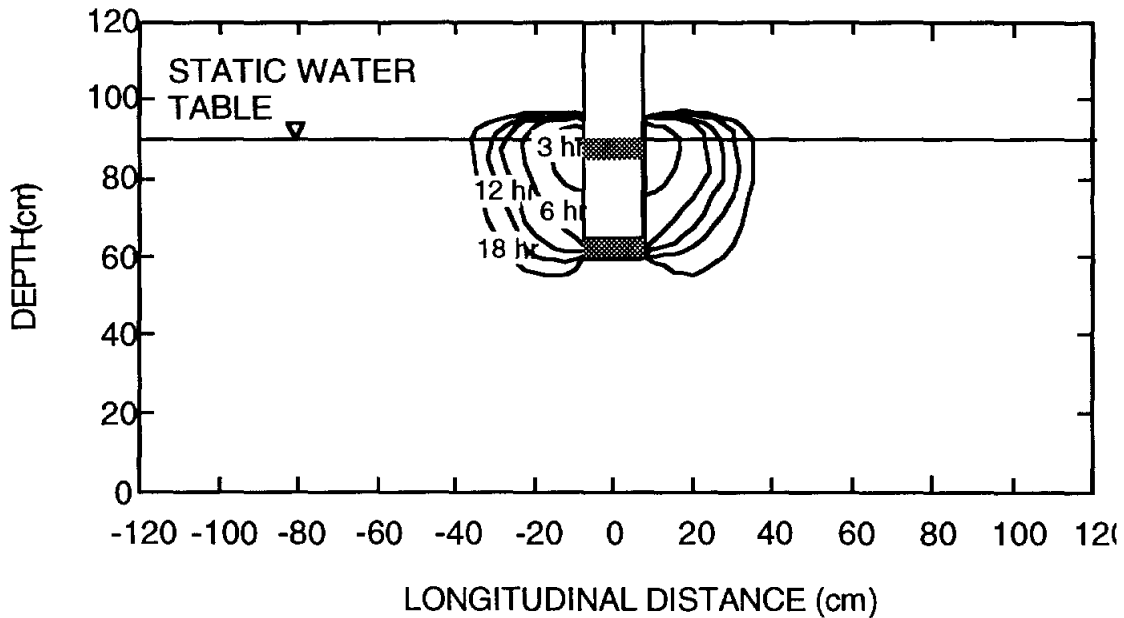


Figure 9. Plume development with no ambient flow and well velocity of 2 m/d for well type 1.

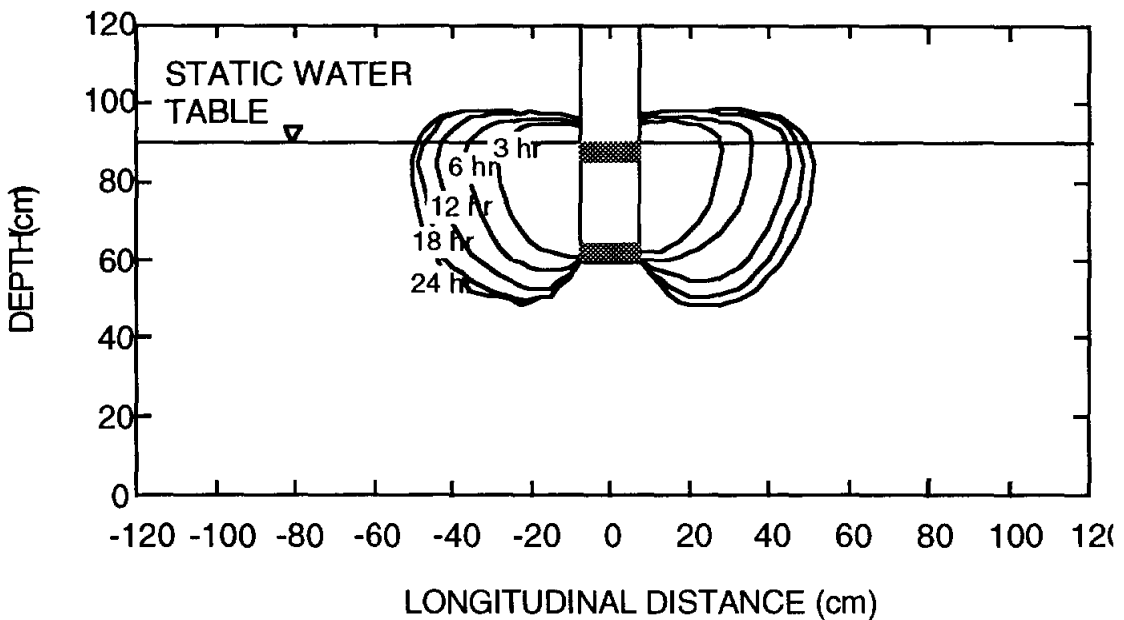


Figure 10. Plume development with no ambient flow and well velocity of 4 m/d for well type 1.

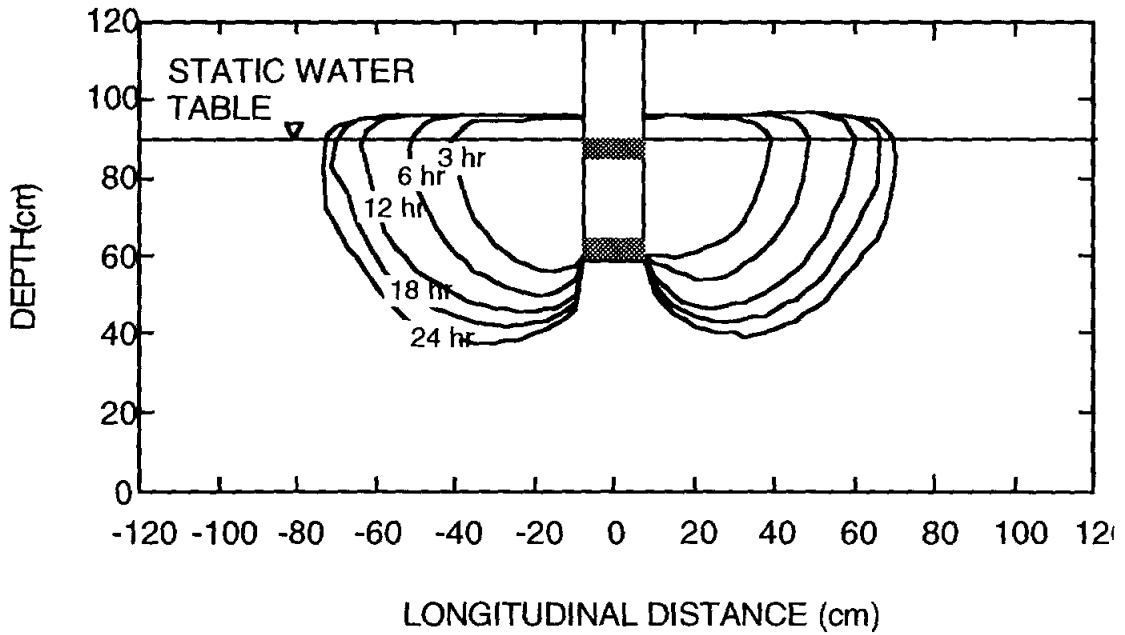


Figure 11. Plume development with no ambient flow and well velocity of 8 m/d for well type 1.

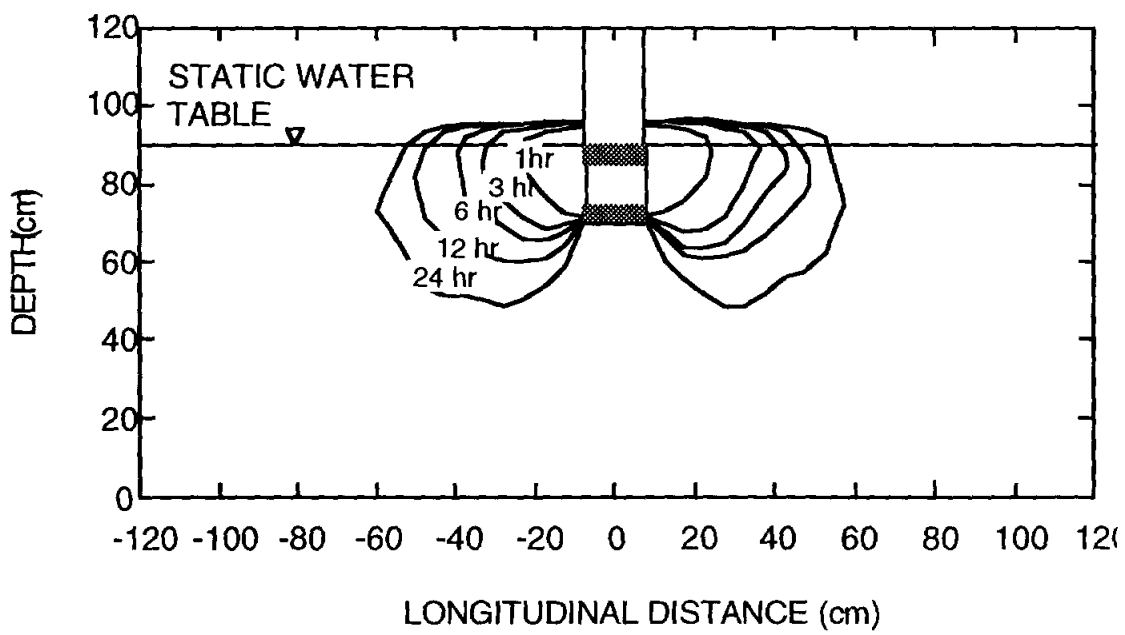


Figure 12. Plume development with no ambient flow and well velocity of 8 m/d for well type 2, Run 1.

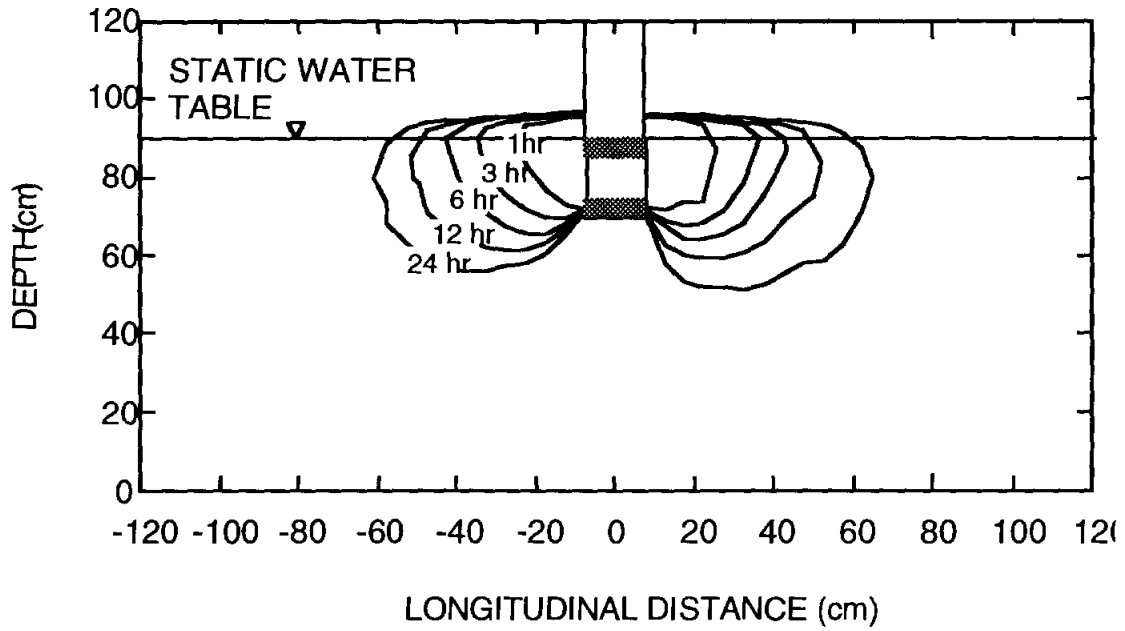


Figure 13. Plume development with no ambient flow and well velocity of 8 m/d for well type 2, Run 2.

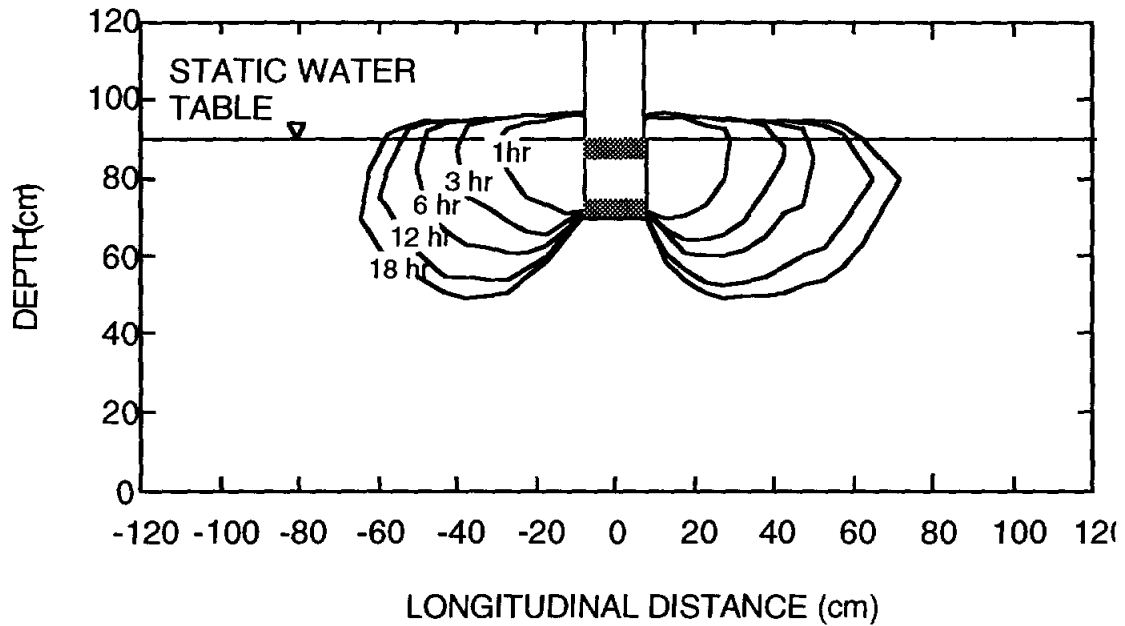


Figure 14. Plume development with no ambient flow and well velocity of 16 m/d for well type 2.

**Table 3. Hydroxide plume diameters for no ambient flow and different pumping rates after 24 hours of continuous RGRW operation.**

Internal well velocity, m/d	Plume diameter, cm
2	50.8
4	83.8
8	135.8

The plumes tended to extend below the bottom of the RGRW. This plume shape would not be noted for a perfectly penetrating well, because the impermeable layer at the bottom of the well would restrict the plume development. Within the time frame of the experiments, this effect was more pronounced at higher well pumping rates.

#### **Well with ambient horizontal ground water flow**

Three sets of experiments were conducted in which the tank was subjected to an ambient horizontal water flow in addition to the recirculation flow in the well. In the first set of ambient flow experiments, the well was operated as before except that water was pumped through the tank to simulate an ambient horizontal flow. The flow extracted from the end of the tank was adjusted to pH 7 by the addition of HCl before it was returned to the head of the tank. A summary of the tested conditions is given in Table 4.

**TABLE 4. Summary of tested conditions with ambient flow; NaOH added to recirculating well.**

Well Type	Ambient ground water velocity	Vertical well velocity
1	2.0 m/d	2.0 m/d
1	1.0 m/d	4.0 m/d
2	1.0 m/d	8.0 m/d
2	1.0 m/d	16.0 m/d

The plume developments for each of the conditions listed in Table 4 are illustrated in Figures 15 through 19. Ambient horizontal flows tended to distort the plumes around the RGRW, with the upstream side of the plume compressed, and the downstream side of the plume elongated. The ambient flow also reduced the extent of the plume below the bottom of the recirculation well.

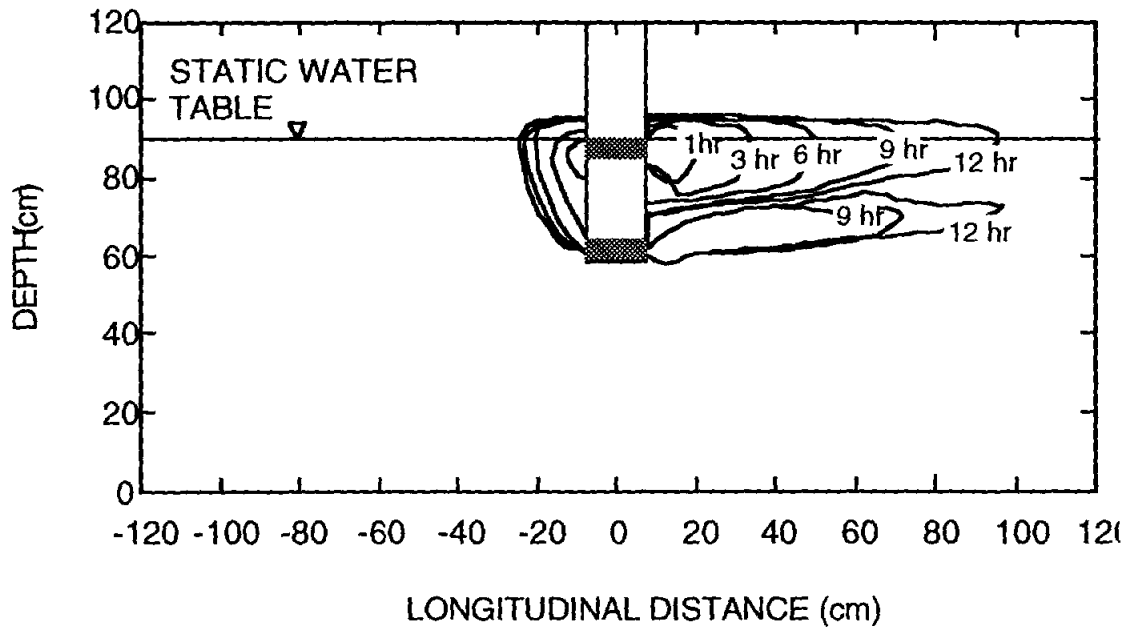


Figure 15. Plume development with 2 m/d ambient flow velocity, 2 m/d internal well velocity, and NaOH added to RGRW for well 1.

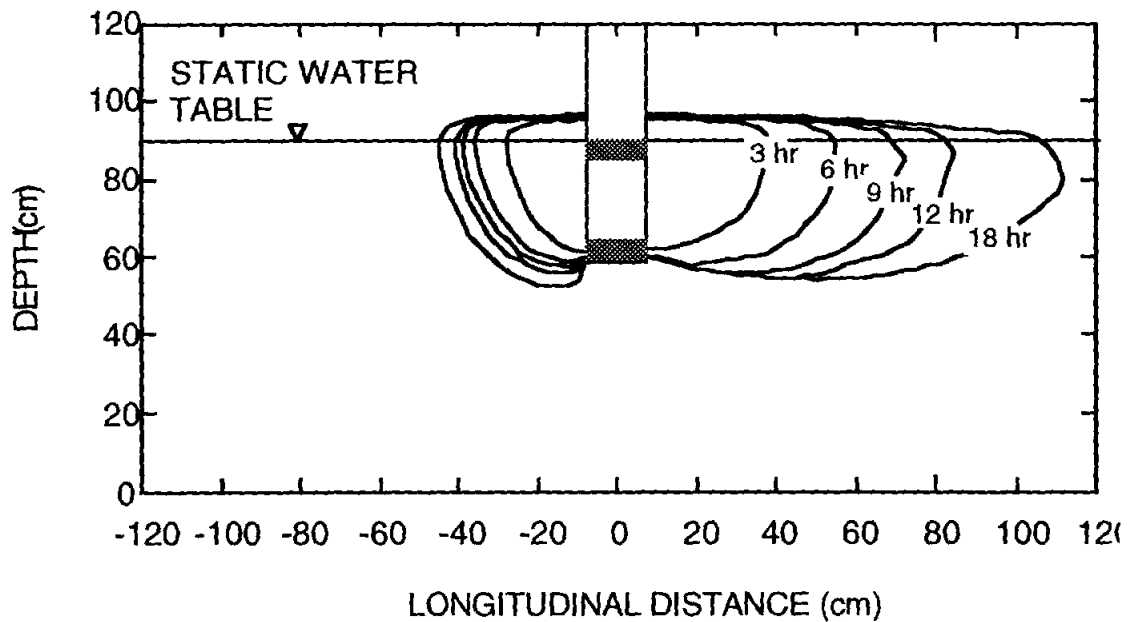


Figure 16. Plume development with 1 m/d ambient flow velocity, 4 m/d internal well velocity, and NaOH added to RGRW for well 1.

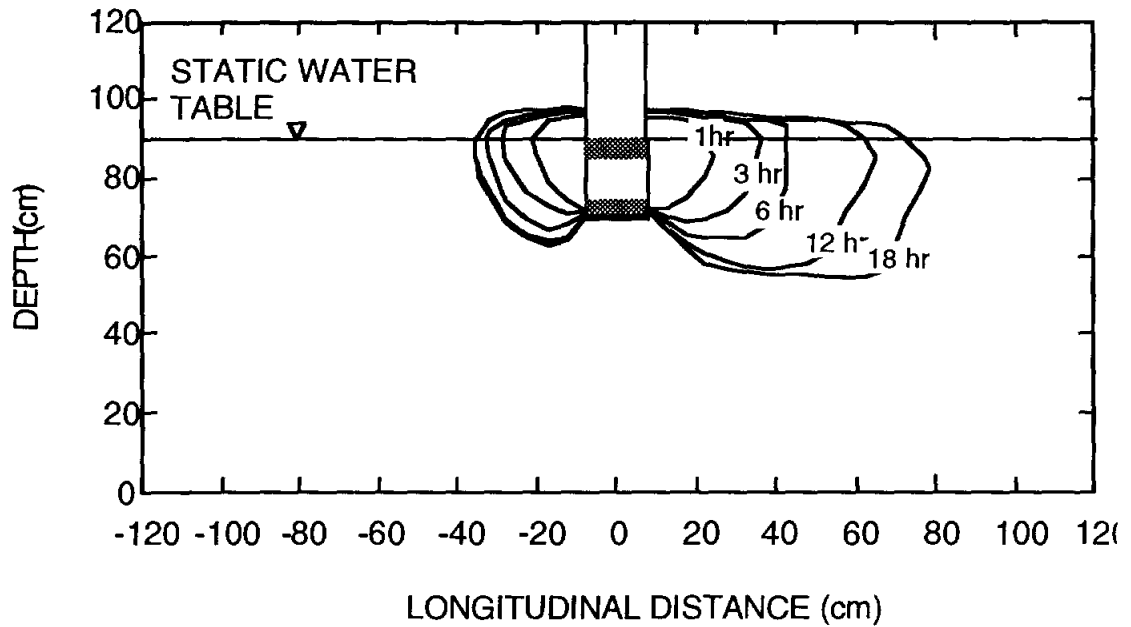


Figure 17. Plume development with 1 m/d ambient flow velocity, 8 m/d internal well velocity, and NaOH added to RGRW for well 2, Run 1.

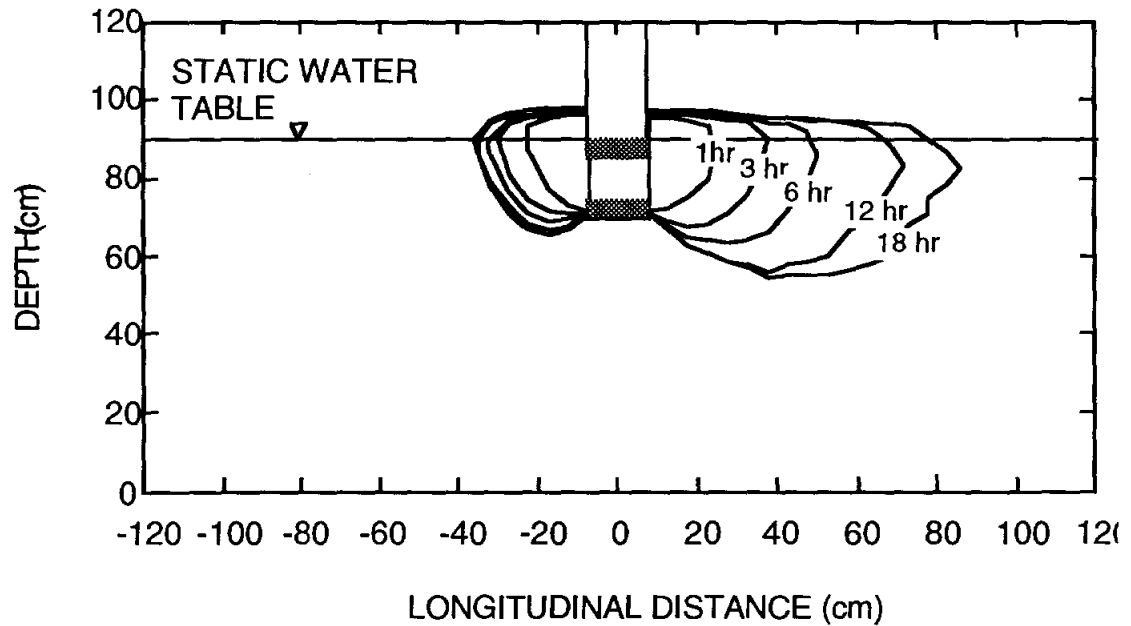


Figure 18. Plume development with 1 m/d ambient flow velocity, 8 m/d internal well velocity, and NaOH added to RGRW for well 2, Run 2.

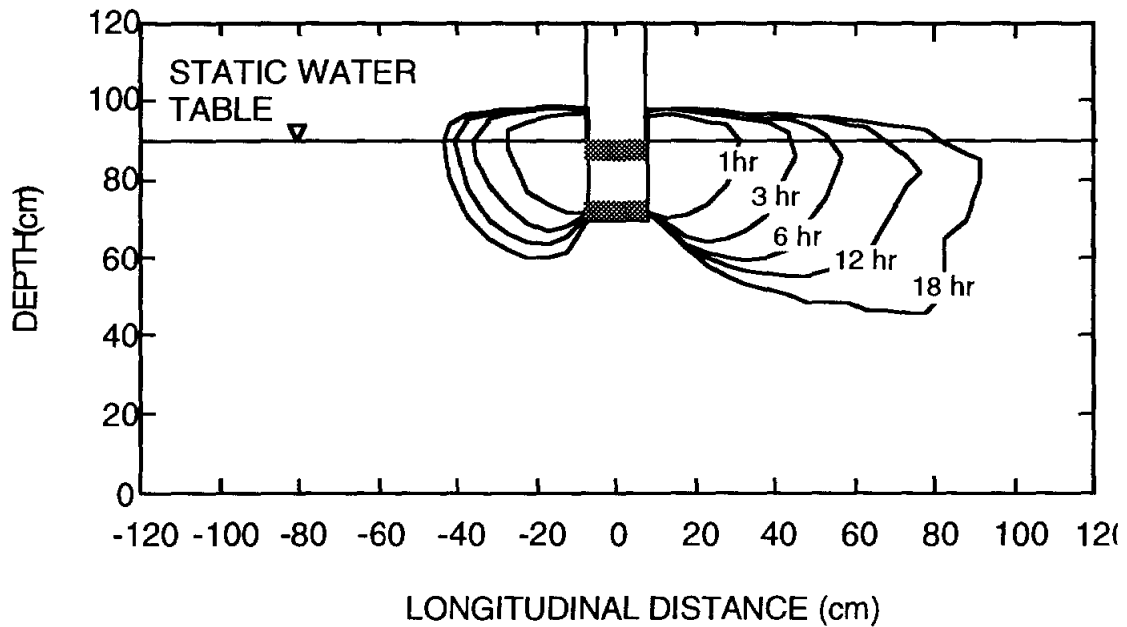


Figure 19. Plume development with 1 m/d ambient flow velocity, 16 m/d internal well velocity, and NaOH added to RGRW for well 2.

### Ambient horizontal flow, depth distributed pollutant

For the next set of experiments, NaOH was added to the water entering at the end of the tank. HCl was added to the wells, so that treatment was simulated by a lowering of the pH, with a corresponding clearing of the NaOH plume by the RGRW. The NaOH was mixed completely into the tank inlet tube, so that there was a uniform distribution of OH<sup>-</sup> ions through the tank depth upstream of the RGRW influence. The system was operated with different well velocities to determine the effectiveness of capture and to identify capture problems that might occur for different combinations of velocities.

**TABLE 5. Summary of tested conditions for ambient flow; NaOH distributed through depth.**

Well Type	Ambient ground water velocity	Vertical well velocity
1	1.0 m/d	4.0 m/d
1	1.0 m/d	8.0 m/d

Typical clearing of the NaOH plume with ambient horizontal flow and NaOH distributed through the depth of the ground water is illustrated in Figures 20 and 21. The NaOH was successfully drawn into the well, and chemically neutralized.

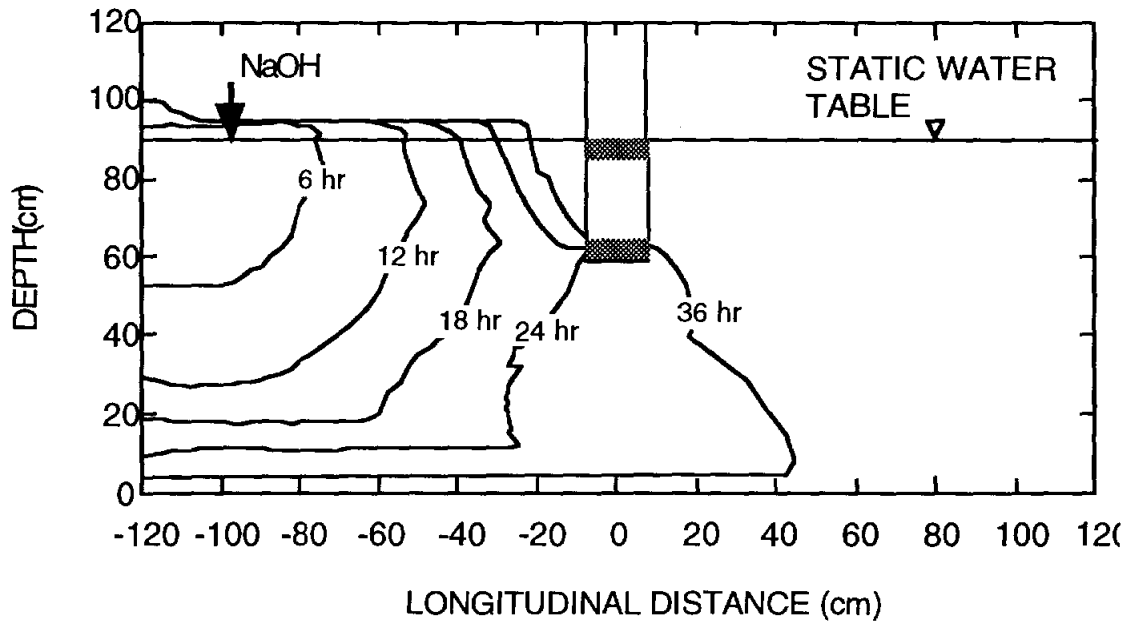


**Figure 20. Plume development with 1 m/d ambient flow velocity, 4 m/d internal well velocity, and NaOH distributed with depth for well 1.**

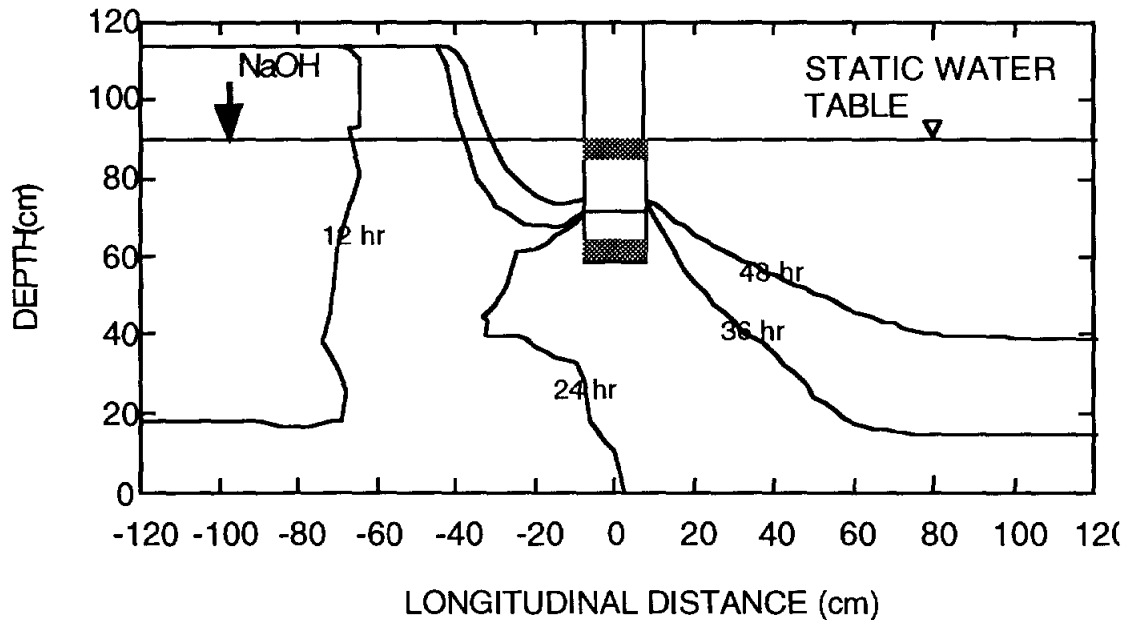


Figure 21. Plume development with 1 m/d ambient flow velocity, 8 m/d internal well velocity, and NaOH distributed with depth for well 1.

### Ambient horizontal flow, surface pollutant

In the third group of ambient flow experiments, NaOH was added at the surface of the ground water just downstream of the ambient flow inlet tube as illustrated in Figure 22. The NaOH formed a surface plume that was carried into the zone of influence of the RGRW. This distribution of pollutant would be typical of a solute that had been applied to the ground water from the surface, such as agricultural source nitrate. Again, hydrochloric acid was added to the injection compartment of the RGRW to simulate treatment. The system was operated under different velocities to evaluate RGRW capture capabilities for surface distributed contaminants and to identify combinations of operating conditions that could influence the efficiency of capture.

**TABLE 6. Summary of tested conditions for ambient flow; NaOH applied at the water table.**

Well Type	Ambient ground water velocity	Vertical well velocity
1	1.0 m/d	4.0 m/d
1	1.0 m/d	8.0 m/d
1	1.0 m/d	12.0 m/d
1	3.0 m/d	4.0 m/d
2	1.0 m/d	8.0 m/d
2	1.0 m/d	16.0 m/d

The plume shapes with ambient horizontal flow and NaOH applied to the surface of the ground water are illustrated in Figures 22 through 28. The NaOH which had been concentrated at the surface was drawn into the ground water to a deeper level than the bottom of the recirculation well. The plume was successfully drawn into the well, and chemically neutralized under all flow conditions studied except the case of 3 m/d ambient ground water velocity. That case is discussed later in this paper.

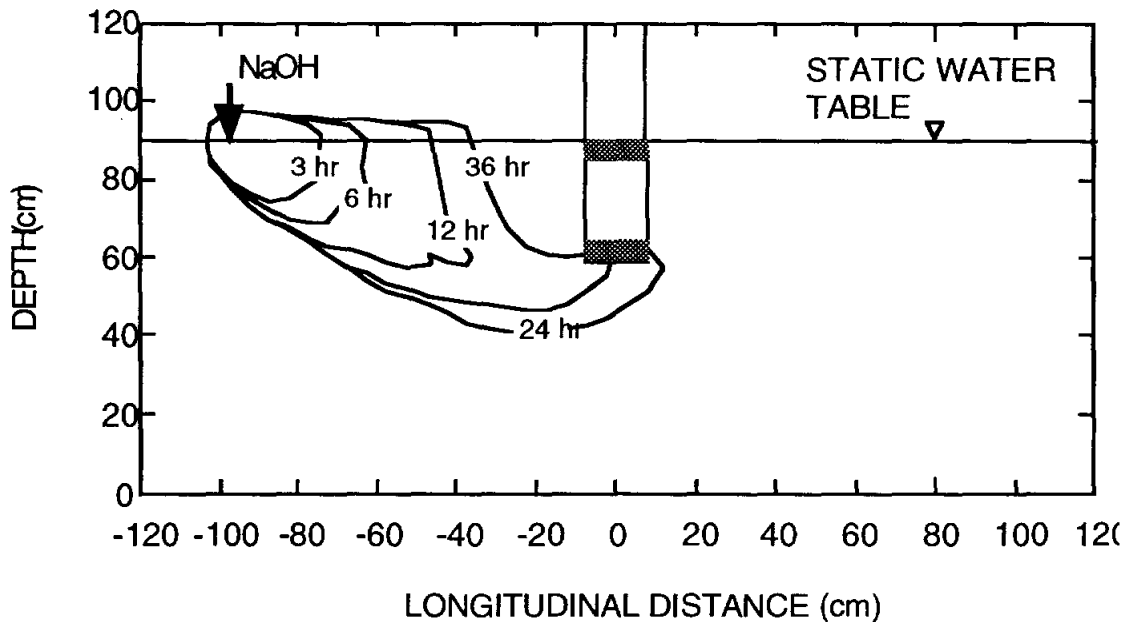


**Figure 22. Plume development with 1 m/d ambient flow velocity, 4 m/d internal well velocity, and NaOH applied at water table with well 1.**

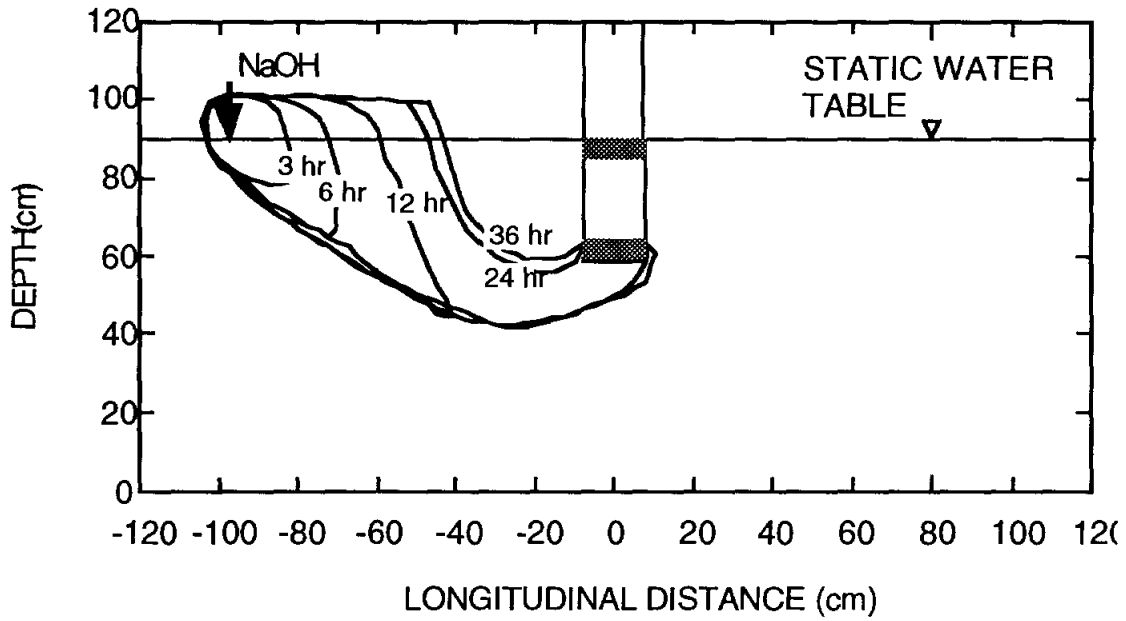


Figure 23. Plume development with 1 m/d ambient flow velocity, 8 m/d internal well velocity, and NaOH applied at water table with well 1.

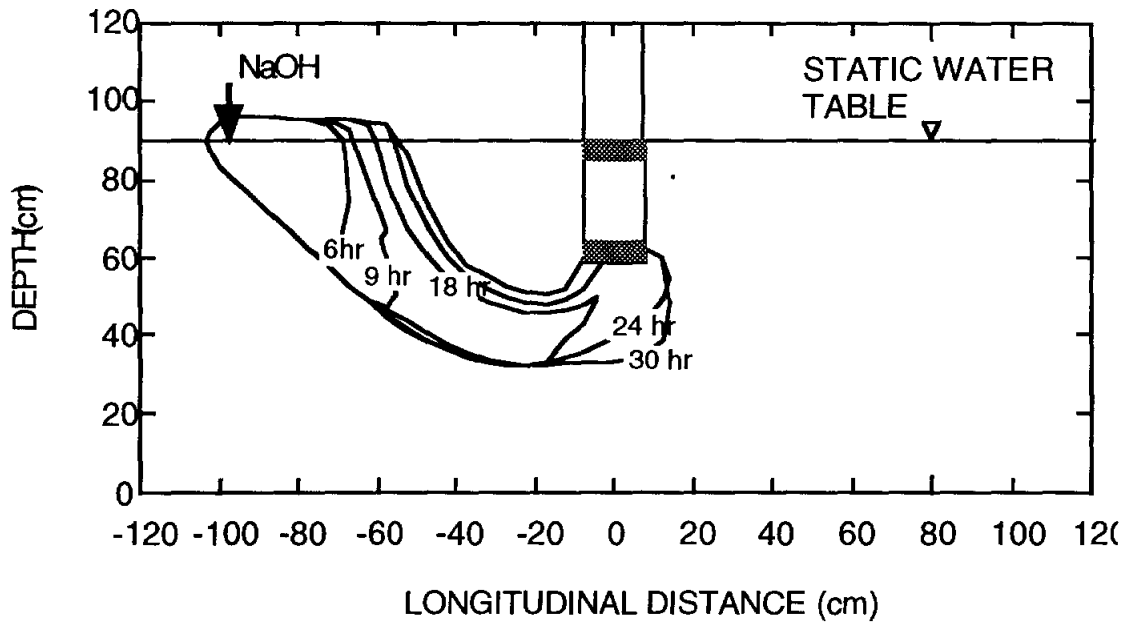


Figure 24. Plume development with 1 m/d ambient flow velocity, 12 m/d internal well velocity, and NaOH applied at water table with well 1.

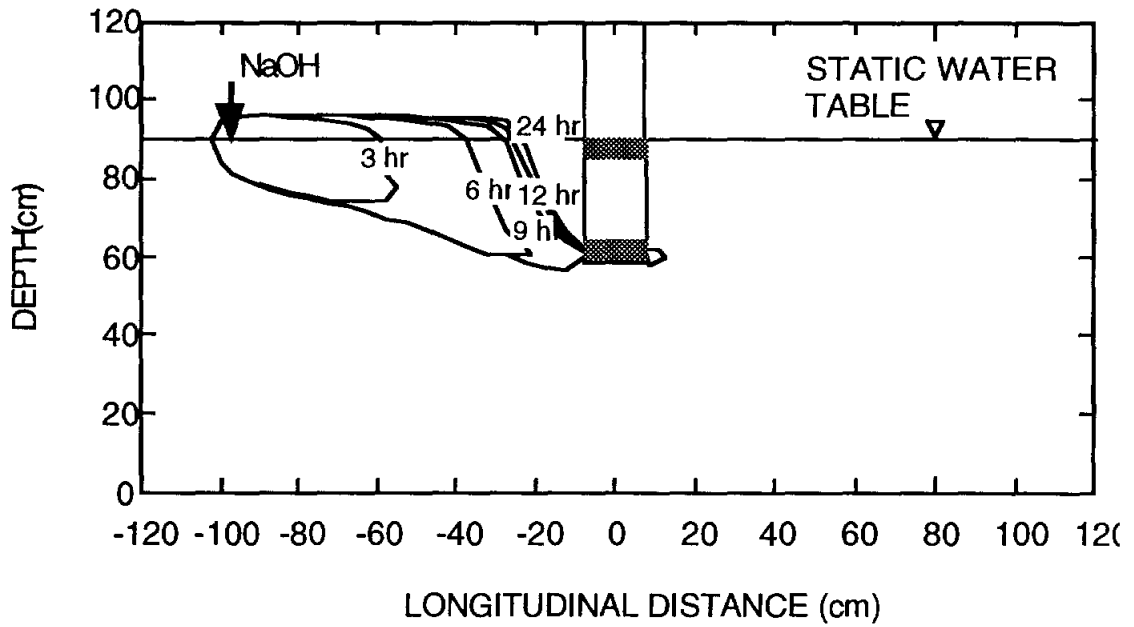


Figure 25. Plume development with 3 m/d ambient flow velocity, 4 m/d internal well velocity, and NaOH applied at water table with well 1.

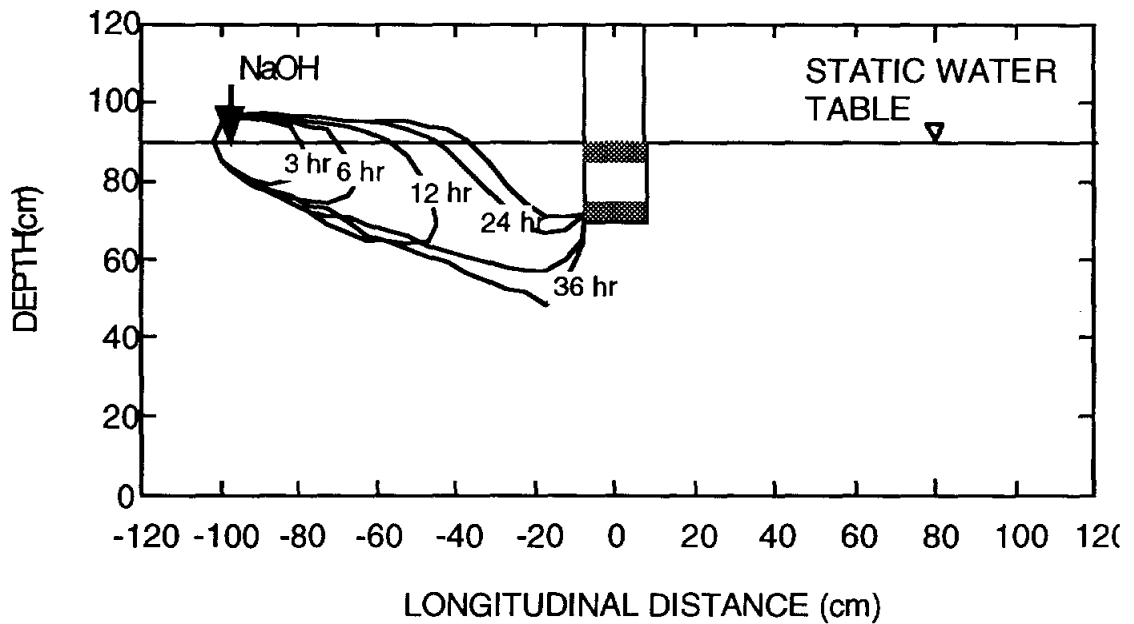


Figure 26. Plume development with 1 m/d ambient flow velocity, 8 m/d internal well velocity, and NaOH applied at water table with well 2, Run 1.

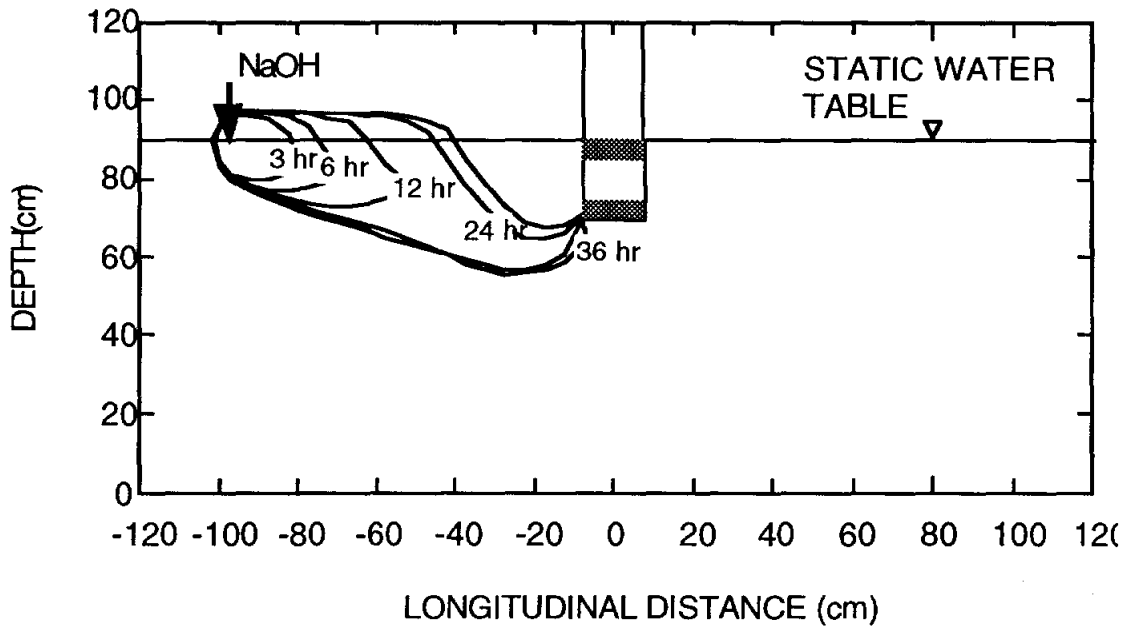


Figure 27. Plume development with 1 m/d ambient flow velocity, 8 m/d internal well velocity, and NaOH applied at water table with well 2, Run 2.

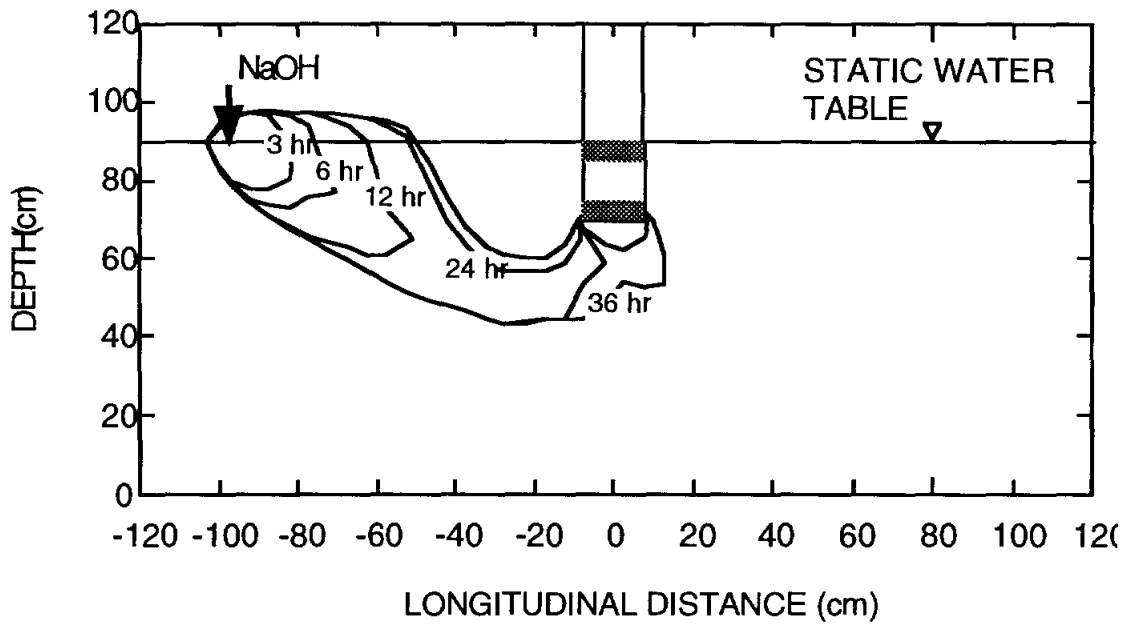
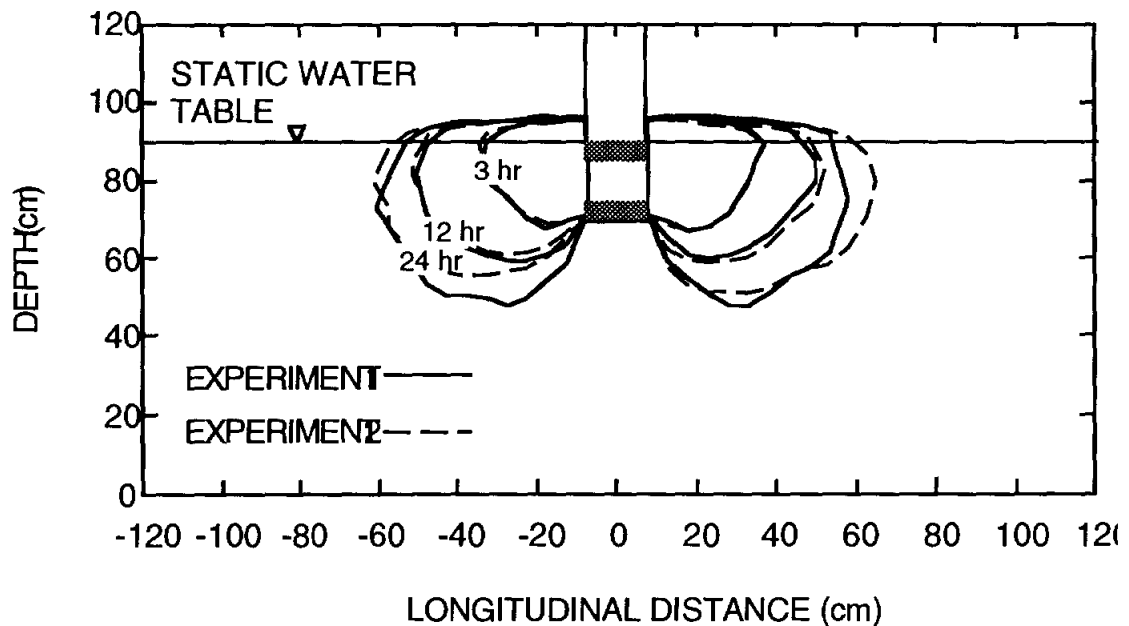


Figure 28. Plume development with 1 m/d ambient flow velocity, 16 m/d internal well velocity, and NaOH applied at water table with well 2.

## Experiment reproducibility and sensitivity

An important consideration in implementing an RGRW system is the robustness of the system, and its sensitivity to small differences in operating conditions. Several of the experiments described above were duplicated in order to test how reproducible the results would be given inevitable differences in the operations due to coarseness of pump controls, etc. The results for two sets of experiments carried out with no ambient horizontal flow and vertical well velocity of 8 m/d are shown in Figures 13 and 14, and compared in Figure 29. Some divergence can be noted in Figure 29, particularly in the plume diameter and depth at longer times in the experiments. The total diameter difference was less than 7 percent at 18 hours into the experiments. Depth below the water table diverged by approximately 12 percent over the same time period. Duplicates of the experiments in which NaOH was added to the RGRW with ambient ground water flow are shown in Figures 17 and 18, and are compared in Figure 30. Duplicate experiments in which NaOH was added to the water table reflected similar divergences, as shown in Figures 26, 27, and 31.



**Figure 29.** Comparison of plumes with no ambient flow, 8 m/d internal well velocity, and NaOH added to RGRW with well 2.

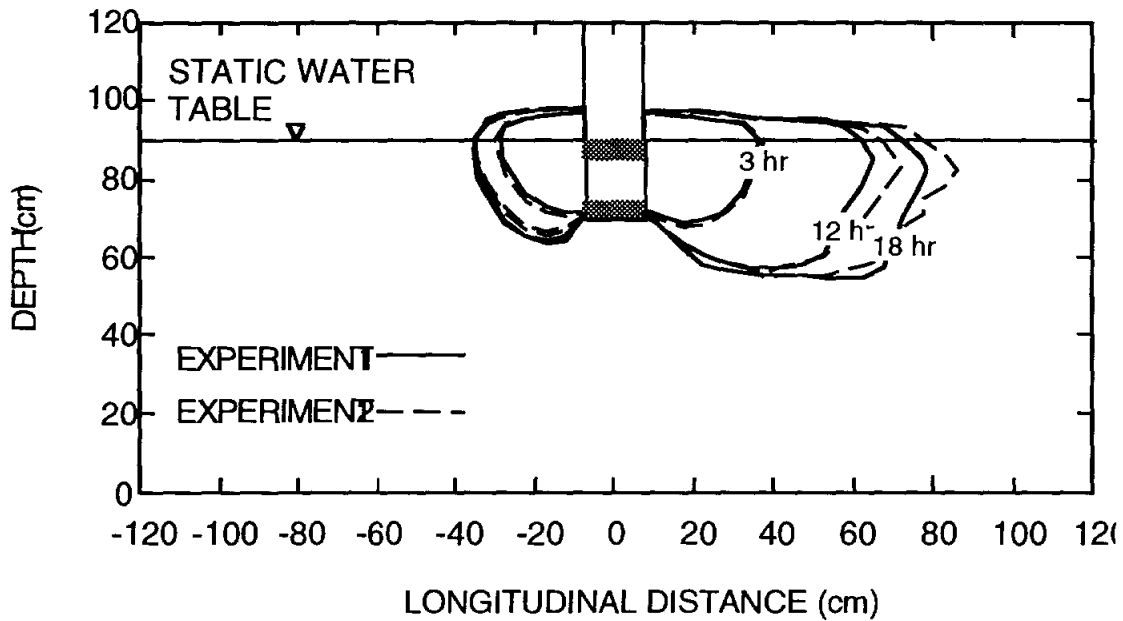


Figure 30. Comparison of plumes with 1 m/d ambient flow velocity, 8 m/d internal well velocity, and NaOH added to RGRW with well 2.

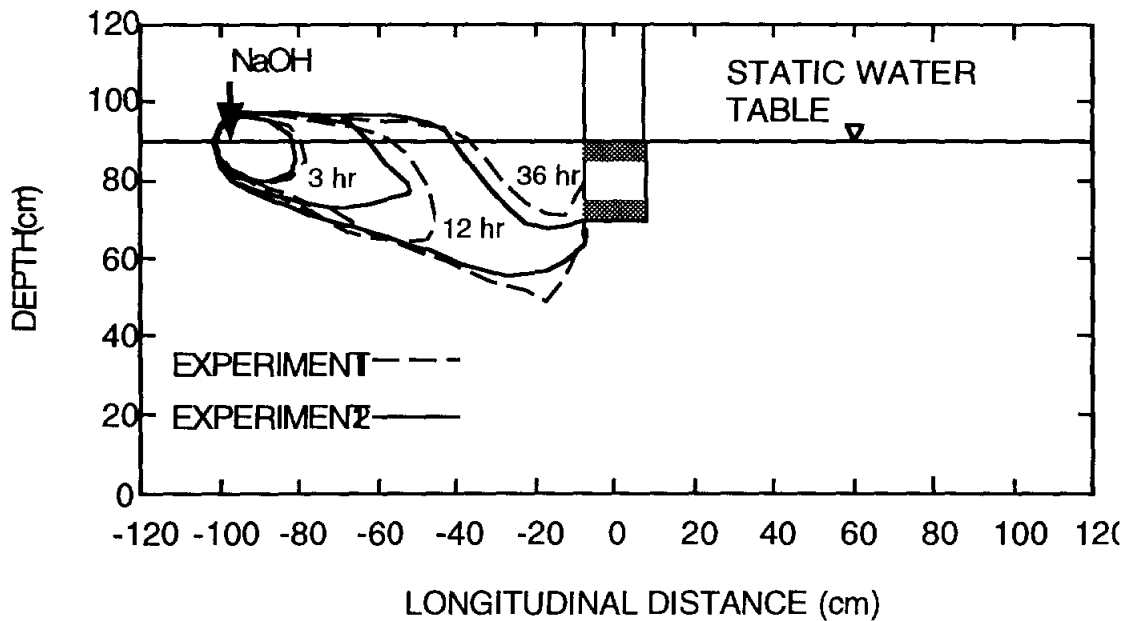


Figure 31. Comparison of plumes with 1 m/d ambient flow velocity, 8 m/d internal well velocity, and NaOH applied at water table with well 2.

Plume development was found to be sensitive to ambient horizontal ground water velocity. Because the sidewalls of the lower withdrawal compartment of the RGRW are open, when the ambient ground water velocity is large relative to the internal well velocity, pollutants

can be swept through the withdrawal compartment without being drawn into the treatment compartment. In the pseudo-two-dimensional experiments reported, the effect is to limit the recirculation to the upgradient side of the well, resulting in development of a secondary plume originating at the downgradient side of the withdrawal compartment.

This blowthrough effect was noted for two of the conditions studied. For RGRW type 1 subjected to an ambient flow velocity of 2 m/d and internal well velocity of 2 m/d, with NaOH added to the treatment compartment of the well, the secondary plume developed as shown in Figure 15. The downgradient reach of the plume was about 20 percent greater than the reach for the experiment shown in Figure 16 after 12 hours. The conditions illustrated in Figure 10 included an ambient flow velocity of 1 m/d, internal well velocity of 4 m/d, and NaOH added to the treatment compartment of the well. There is less difference in plume reach between the two conditions than might be expected because the effects of higher velocity and possible blowthrough are partially offset by the faster plume development noted with higher internal well velocity.

The other studied condition for which some blowthrough was noted is illustrated in Figure 25. In that case, the ambient ground water velocity was 3 m/d, with internal well velocity of 4 m/d and NaOH applied to the ground water table upgradient of the RGRW. A small secondary plume was noted on the downgradient side of the withdrawal compartment after 24 hours. Pollutant approaching the RGRW near the surface of the ground water is expected to be typical of a large number of applications for RGRW systems, so that the development of a secondary plume in this case is of some concern. While the secondary plume is small in this case, other combinations of ambient and internal well velocities may result in contaminant being submerged into the ground water, rather than being removed.

## NUMERICAL MODEL

A numerical model was developed to provide a tool to predict the long term operation of a RGRW system. The model couples the solution of a two-dimensional unsaturated/saturated flow equation with the solution of a two-dimensional contaminant transport equation. Unsaturated and saturated flow conditions were incorporated into the model because the ground water surface rises above the ambient flow condition level in the vicinity of the RGRW during pumping. Generally, the water rise in the soil at locations distant from the well was minor, and could be ignored. The model was solved using a standard finite difference technique and results were compared with those of a commercially available contaminant transport model [Yeh, 1987 and 1990]. The bases of the flow and transport model development are described below. Results of the model calibration to the experimental tank results and a comparison of modeled with experimental results also are presented.

## MODEL DEVELOPMENT

The basic numerical model consists of flow and transport equations. The equation used to describe flow through saturated and unsaturated porous media can be derived from Darcy's law and the equation of continuity [Bear and Verruijt, 1987]:

$$\nabla \cdot \left[ \frac{K(\theta)}{\rho g} (\nabla P_c + \rho g \nabla z) \right] + Q = \left( S_{op} + \frac{d\theta}{dP_c} \right) \frac{\partial P_c}{\partial t} \quad (1)$$

where  $K(\theta)$  is the unsaturated hydraulic conductivity of water;  $\theta$  is the water content;  $P_c$  is the suction pressure;  $\rho$  is the density of water;  $g$  is the gravitational acceleration;  $z$  is the potential head;  $Q$  is the flow rate of source or sink;  $S_{op}$  is the specific yield;  $\frac{d\theta}{dP_c}$  is the water capacity; and  $t$  is time.

The hydraulic conductivity,  $K(\theta)$  depends on the water content and can be expressed by Mualem's equation [Mualem, 1976] as:

$$\kappa(\theta) = \kappa_s \theta_e^{1/2} \left[ 1 - \left( 1 - \theta_e^{m/(m-1)} \right)^{(m-1)/m} \right]^2 \quad (2)$$

where  $\kappa(\theta)$  is the hydraulic conductivity;  $\kappa_s$  is the saturated hydraulic conductivity;  $m$  is an empirical constant; and  $\theta_e$  is the effective water content.

Water content in the unsaturated zone can be expressed as a function of capillary pressure [Van Genuchten, 1980]:

$$\theta_e = \frac{\theta - \theta_r}{\theta_s - \theta_r} = \left[ \frac{1}{1 + (\alpha P_c)^m} \right]^{(m-1)/m} \quad (3)$$

where  $\theta_r$  is the residual water content;  $\theta_s$  is the saturated water content, *i.e.*, porosity; and  $\alpha$  is an empirical constant.

Differentiation of Eq. (3) gives:

$$\frac{d\theta}{dP_c} = \frac{\alpha(m-1)(\theta_s - \theta_r)(\alpha P_c)^{(m-1)}}{\left[ 1 + (\alpha P_c)^m \right]^{(2m-1)/m}} \quad (4)$$

Contaminant transport is described by the transport equation:

$$R\theta \frac{\partial C}{\partial t} = -\nabla \cdot \theta(-D\nabla C + VC) + Q(C - C^*) + \theta\rho S \quad (5)$$

where  $R$  is the retardation factor;  $C$  is the solute concentration;  $V$  is the ground water velocity;  $D$  is the hydrodynamic dispersion coefficient;  $C^*$  is the solute concentration at the source; and  $S$  is the rate of solute production.

The hydrodynamic dispersion coefficient is expressed in terms of longitudinal and transverse dispersivities [Bear and Verruijt, 1987]:

$$D_{ij} = \alpha_T v \delta_{ij} + (\alpha_L + \alpha_T) \frac{v_i v_j}{v} \quad (6)$$

where  $i, j$  are the longitudinal and transverse directions;  $\alpha_T$  and  $\alpha_L$  are the transverse and longitudinal dispersivities, respectively; and  $v_i$  and  $v_j$  are the average ground water velocities in the subscripted directions. The effects of molecular diffusion are assumed to be negligible.

Basic assumptions made in developing the model include: i) the porosity and density of the aquifer material are homogeneous and constant in time; ii) the coefficients of longitudinal and transverse dispersivity are homogeneous and isotropic with respect to aquifer material; iii) the effects of density, viscosity, and temperature variations are negligible; and iv) the effects of chemical reactions on the ionic strength of the solution, the fluid properties, and the aquifer properties are negligible.

### **SOLUTION TECHNIQUE**

The tank was modeled on a 50 by 24 node grid with 5 cm between nodes in two dimensions. Boundary conditions were specified at the well and along the edges of the tank. Eqn. 1 was solved using a fully implicit finite difference technique. Development of the finite difference equations and iterative alternating direction implicit solutions have been presented in various publications, e.g., Bear and Verruijt [1987], and will not be repeated here.

The method of characteristics was used to solve the contaminant transport equation, Eqn. 5. The two-dimensional material derivative of contaminant concentration may be written as:

$$\frac{dc}{dt} = \frac{\partial c}{\partial t} + \frac{\partial c}{\partial x} \frac{dx}{dt} + \frac{\partial c}{\partial y} \frac{dy}{dt} \quad (7)$$

where  $x$  and  $y$  are horizontal and vertical Cartesian coordinates.

In Eqn 7,  $\frac{dx}{dt}$  and  $\frac{dy}{dt}$  correspond to flow velocity components,  $v_x$  and  $v_y$  in the  $x$  and  $y$  directions, respectively.

$$v_x = \frac{dx}{dt} \quad (8)$$

$$v_y = \frac{dy}{dt} \quad (9)$$

Substituting into Eqn. 5,

$$\frac{dC}{dt} = \frac{1}{R\theta} \left[ \frac{\partial}{\partial x_i} \left( D_{ij} \frac{\partial C}{\partial x_j} \right) \right] + E \quad (10)$$

where  $E$  includes the other terms of Eqn 5. The solution of Eqn. 8 can be represented by  $x = x(t)$ ,  $y = y(t)$ , and  $C = C(t)$ , which are referred to as the characteristic curves of Eqn 5. With given solutions of Eqns 8, 9, and 10, the solution of Eqn 5 can be obtained by following the characteristic curves. This method has been successfully applied in various models, e.g., Konikow and Bredehoeft [1978].

## PARAMETER ESTIMATION AND CALIBRATION

The numerical model of the experimental tank was calibrated to the conditions of plume development without ambient horizontal ground water flow and internal well velocity of 4 m/d. The resulting predicted NaOH plume is compared with the measured plumes in Figure 32. There is excellent agreement between the predicted and measured plumes.

The dynamic viscosity and density of water were assumed to remain constant throughout the tank. The retardation coefficient for nitrate in the soil was assumed to be 1.0. Values of the adjusted calibration parameters are shown in Table 7. Dispersivities are empirical factors that describe the mixing effect in the direction of flow (longitudinal) and normal to the direction of flow (transverse). Generally, they are reported to differ by approximately an order of magnitude [Bear and Verruijt, 1987]. The adjusted parameters were employed in subsequent simulations without further adjustments.

Hydroxide ion ( $\text{OH}^-$ ) was used as the contaminant in this study, so source concentrations are expressed in terms of pH. The source input at the well was fixed at pH 12, and the concentration of contaminant at other locations was calculated by the transport model. The pH 9 contour is plotted as the boundary of the RGRW capture zone, and compared with the extent of the visible plume as measured in the experiments.

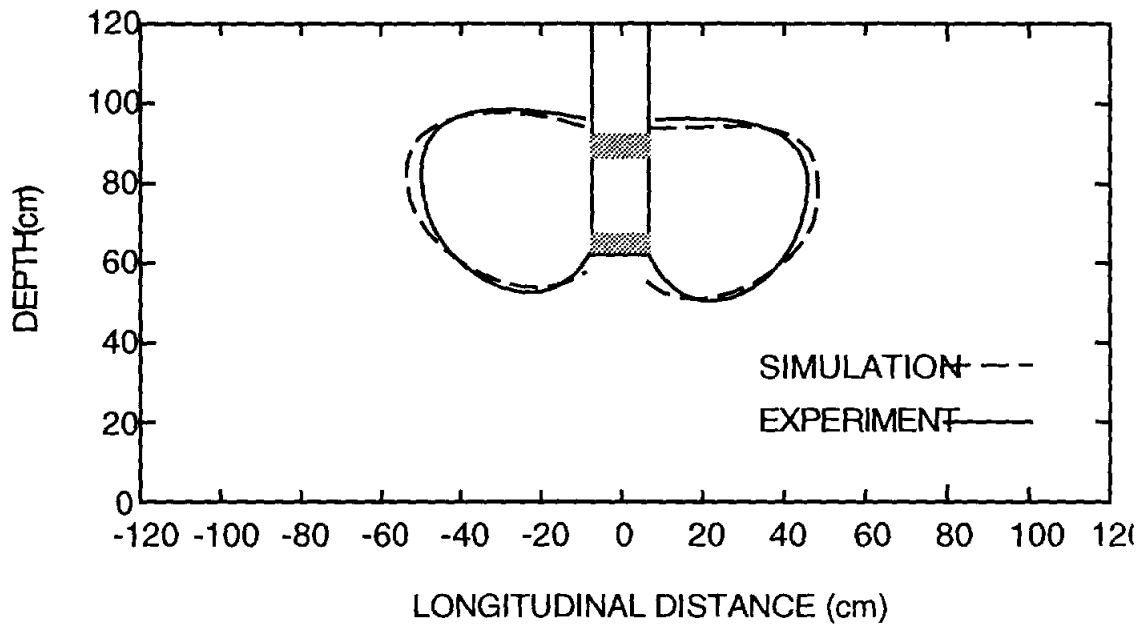


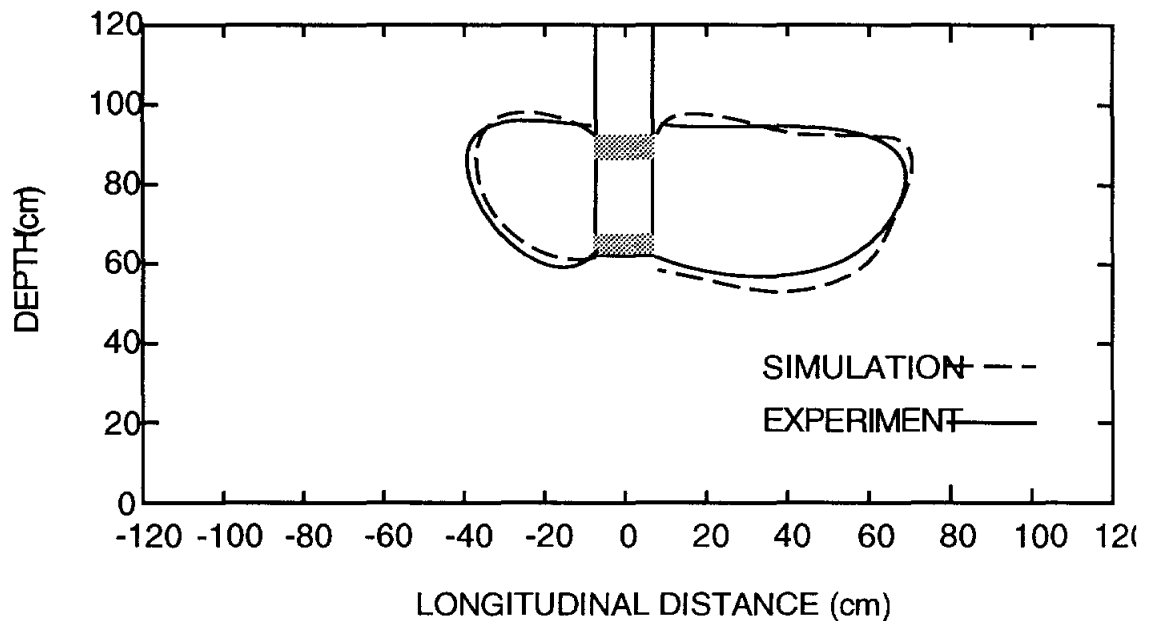
FIGURE 32. Model calibration basis and results: NaOH plume (pH=9) with stationary ground water and internal well velocity of 4 m/d.

TABLE 7. Model parameter values estimated by calibration

Property	Units	Value
longitudinal dispersivity ( $\alpha_1$ )	cm	1.2
transverse dispersivity ( $\alpha_t$ )	cm	0.12
residual water content ( $\theta_r$ )		0.1

## NUMERICAL RESULTS

The plume shape with ambient horizontal flow of 1 m/d and internal well velocity of 4 m/d after 24 hours is compared with the plume predicted by the model in Figure 30. Again, there is excellent agreement between the predicted and measured plumes. The agreement shown in Figure 30 is typical for all experiments listed in Table 4.



**FIGURE 30. NaOH plume (pH=9) after 24 hours with ambient ground water velocity of 1 m/d and internal well velocity of 4 m/d.**

Measured plumes are compared with model predictions in Figures 31 and 32 for typical experiments of removal of depth-distributed pollutant and pollutant applied to the ground water surface, respectively. The agreement shown in these figures also is typical for all experiments reported with these conditions, as described in Tables 5 and 6.

For the cases in which the NaOH was distributed with depth in the ground water, the agreement between the measured and predicted plumes was again excellent except at the lower downstream end.

For the cases in which the NaOH was added to the surface of the ground water, the agreement between the measured and predicted plumes was not as good as for the other cases. The most significant divergence between the plumes appears to be that the model predicted that the entire pollutant plume would be drawn into the upstream side of the RGRW. In the experiments, a substantial portion of the plume was drawn into the downstream side of the well. A possible explanation for this phenomenon is that head losses in the upstream intake to the well were higher than as modeled. Adjustments to the model parameters to increase the upstream intake headloss relative to the downstream intake headloss resulted in the revised simulated plume prediction shown in Figure 32.

Agreement was much better than for the initial simulation.

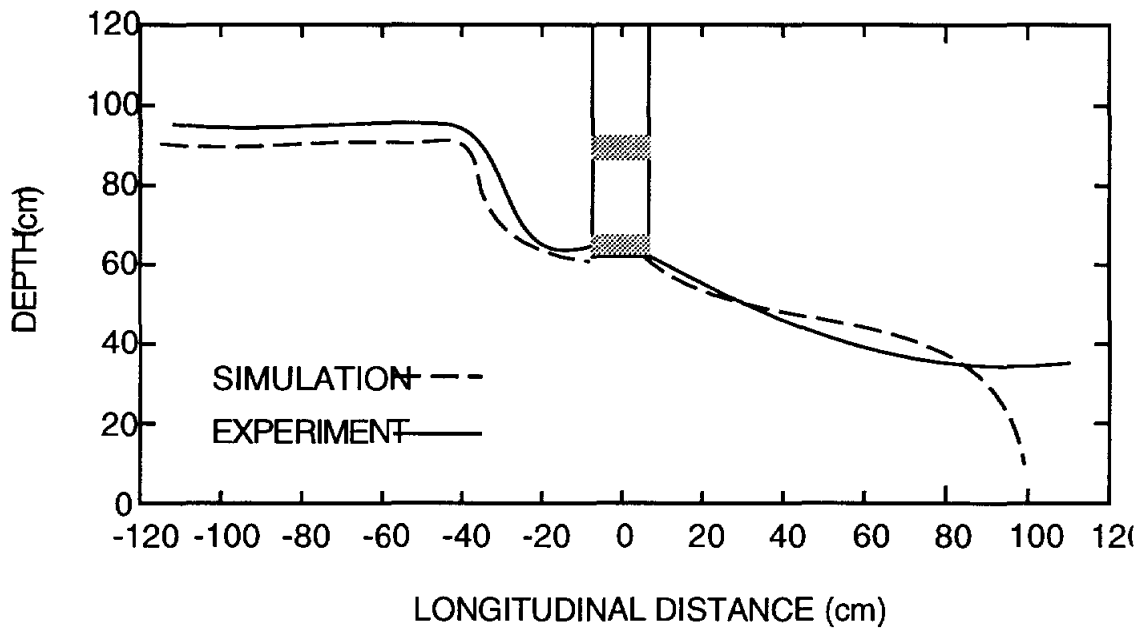


FIGURE 31. NaOH plume (pH=9) after 48 hours with NaOH distributed through depth of ground water, ambient ground water velocity of 1 m/d, and internal well velocity of 8 m/d.

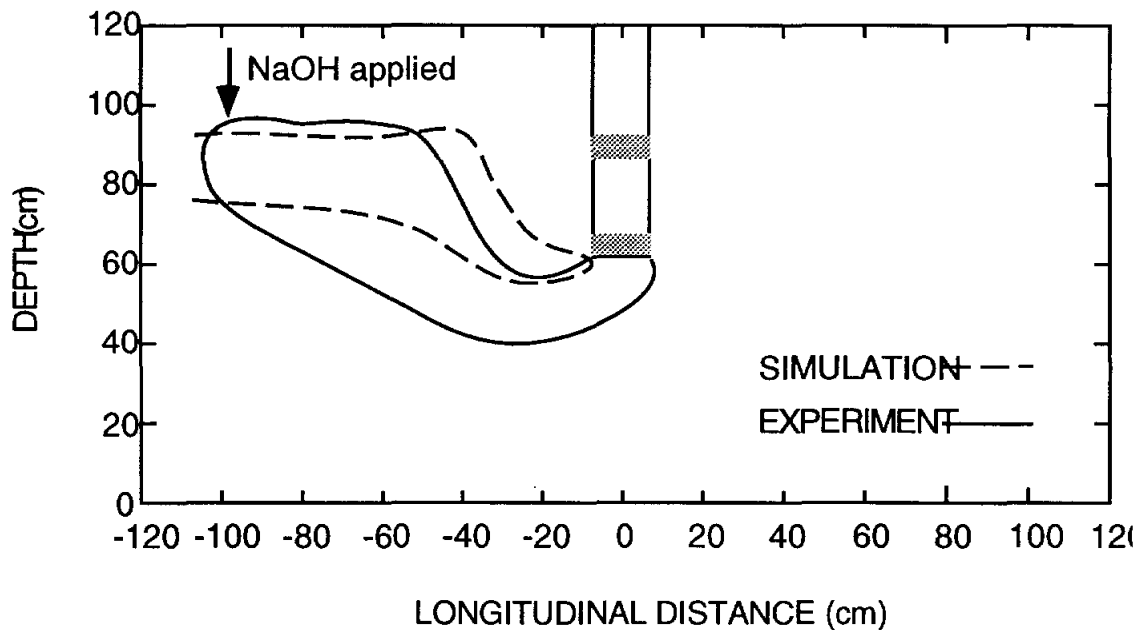


FIGURE 32. NaOH plume after 24 hours with NaOH applied at surface of ground water, ambient ground water velocity of 1 m/d, and internal well velocity of 8 m/d.

Numerical model results for the experiments are shown in Appendix A of this report.

## CONCLUSIONS

In the original proposal, the goals of this research project were stated as:

- 1) to demonstrate the feasibility of protecting a drinking water well from migrating nitrate contamination with the treatment well system;
- 2) to evaluate critical factors in the design and placement of treatment wells;
- 3) to develop control systems and operations strategies for the treatment well-drinking well pairs; and
- 4) to develop a computer-aided design procedure, including a software package, for use by environmental engineers in applying the systems.

We believe that we are well on the way to accomplishing these goals. Thus far, our research has been focused primarily on the hydraulics of the well system. Based on our experimental and numerical results, we can conclude that

- Recirculating ground water remediation wells are a promising method for treating ground water contaminants in the soil. We have demonstrated that the RGRW system can be effective for intercepting migrating pollutants, including conservative pollutants such as nitrate as well as non-conservative sorbing pollutants that tend to adsorb or move into the soil phase.
- The experimental results reported are for a very homogeneous and isotropic soil. Such a system is unlikely to be encountered in the field. While it is impractical to introduce substantial anisotropy in the experimental system described, field experiments should be instituted following this project to confirm results of the numerical analysis of anisotropy that are planned for the second year of the project.
- Experimental analysis of the wells in a pseudo-two dimensional tank showed the well operations to be relatively robust, with some sensitivity to small fluctuations. The wells were experimentally demonstrated for perfectly and imperfectly penetrating wells. It is important that the wells are shown to work for imperfectly penetrating conditions, because the vast majority of applications will involve imperfectly penetrating wells.

- The tests reported here suggest that the radii of influence of the wells are affected by the well internal velocities (pumping rates), contrary to conclusions drawn by previous researchers, at least for the time periods tested.
- Carry-through of pollutant through the well intake chamber and back into the aquifer downgradient of the well can occur in high ambient ground water velocities. The effect would be worse in the pseudo-two dimensional system used for these experiments, and can be eliminated by increasing internal well velocities. The increase in well velocity will result in shorter detention times in the treatment chamber of the well, possibly reducing the degree of pollutant removal. Larger well diameters should correct this problem. However, the practicality of these systems at high ground water velocity must be questioned.
- Numerical models of the system were effective in estimating plume shapes and capture efficiencies.

## **ACTIONS FOR THE COMING YEAR**

The research reported constitutes the first year of a two year study. In the second year of the study, the biological nitrate removal system will be introduced into the wells. Already, we are developing cultures of denitrifying bacteria and collecting data on their growth and performance characteristics for use in the experiments.

In the coming year, we will be conducting experiments within the treatment wells to determine their operational characteristics and treatment efficiency ranges, and to identify the operational and design parameters that can be affected to optimize the treatment well performance. We will be conducting numerical as well as laboratory experiments. The numerical experiments will include modeling of the effect of soil anisotropy and heterogeneity on capture zone and treatment efficiency.

In addition, we will be conducting preliminary experiments to identify the interactions of the biological removal system with the well hydraulics. Increased headloss at the outlet screens may result from precipitation of oxidized chemicals caused by the treatment process or from particulate material pulled into the well from the surrounding aquifer. Particulate material that migrates through soil pores to enter the well with the ground water is expected to pass out of the well and back through the soil pores. A removable microscreen could be installed at the well exit, and cleaned periodically as head loss at the exit increases.

Another potential cause for headloss increase may be filtering of microorganisms or microbial growth in the well exit or surrounding soil. Filtering of microorganisms might be controlled by providing a clarification zone in the well. Growth of microorganisms in the exit and surrounding soil can be controlled by minimizing the concentration of organic material in the effluent of the treatment well. Filtering and growth of microorganisms at soil interfaces is a common occurrence in on-site wastewater disposal systems. The fouling is seldom complete, but results in an increased resistance.

Because the concentrations of organic material in the treatment well are expected to be much less than the concentration of organics in septic tank effluent, microbial fouling is expected to result in a minor increase in head loss through the well exit. Flow could be maintained by increasing the pump head. The effect on biological treatment in the well would be

expected to slightly improve the treatment because the increase in head loss should increase the depth of water in the well and therefore the hydraulic retention time in the well.

Another possible interaction between the treatment system and the well and aquifer hydraulics is that of blinding of the soil pores by gases produced from the denitrification process. Biological denitrification involves conversion of nitrate to nitrogen gas products, principally  $N_2$ . If the denitrification occurs in the soil pores, then the gases may form bubbles that can become entrapped in the soil pores, preventing ground water from flowing through those pores, and altering the well hydraulics.

In addition to investigating these aspects of the biological treatment system, we will incorporate treatment performance modules into the RGRW hydraulics and transport models that we have developed. The design/operational model package will be completed, with user interface.

We also intend to submit papers and make presentations on the hydraulics and biological remediation aspects of this project. We presented some hydraulic results to the AGU Fall 1993 meeting in San Francisco, California in December [Stallard et al, 1993]. We intend to submit an abstract and make a presentation of the biological treatment system at the AGU Spring 1994 meeting in Baltimore, Maryland in May. In addition, we have completed one paper for submission to an engineering journal, and will be completing at least one more in the coming year.

The RGRW system has received a great deal of interest both inside Texas and at a national level. The project has been featured in two issues of the Texas Water Resources Institute newsletter and in the Texas A&M Department of Civil Engineering newsletter. It will be featured on the cover of an upcoming issue of *U. S. Water News*.

## REFERENCES

- Bear, J. and A. Verruijt. 1987. *Modeling Ground water Flow and Pollution*. D.Reidel Publishing Company,
- Coyle, J., H. Borchers, and R. Miltner. 1988. *Control of volatile organic contaminants in ground water by in-well aeration*. U. S. Environmental Protection Agency. EPA 600/S2-888/020.
- Herrling, B., and W. Buermann. 1990. A new method for in-situ remediation of volatile contaminants in ground water - Numerical simulation of the flow regime. In *Computational Methods in Subsurface Hydrology*, G. Gambolati, A. Rinaldo, C. A. Brebbia, W. G. Gray, and G. F. Pinder (Eds.). Springer. Berlin. pp 299-304.
- Herrling, B., J. Stamm, and W. Buermann. 1991. Hydraulic circulation system for in situ bioreclamation and/or in situ remediation of strippable contamination. In *In Situ Bioreclamation*, R. Hinchey and R. Olfenbuttel (Eds). Butterworth-Heinemann. Stoneham, MA, 173-195.
- Herrling, B., W. Buermann, and J. Stamm. 1991. In situ remediation of volatile contaminants in ground water by a new system of 'vacuum-vaporizer-wells'. In *Subsurface Contamination by Immiscible Fluids*, K. U. Weyer (Ed). A. A. Balkema. Rotterdam.
- Konikow, L., and J. Bredehoeft. 1978. Computer model of two-dimensional solute transport and dispersion in ground water, Ch. 2, Book 7, *Techniques of Water Resources Investigations of the USGS*, Washington, D. C.
- MacDonald, T., and P. Kitanidis. 1993. Modeling the free surface of an unconfined aquifer near a recirculation well. *Ground Water* 31:774-780.
- Mualem, Y. 1974. A new model for predicting the hydraulic conductivity of unsaturated porous media, *Water Resour. Res.* 10: 1207-1215.
- Spalding, R., and M. Exner. 1993. Occurrence of nitrate in ground water—a review, *J. Environ. Qual.* 22:392-402
- Van Genuchten, M. 1980. Th., Closed form equation for predicting the hydraulic conductivity of unsaturated soil. *Soil Sci. Soc. Am. J.* 44: 892-898.
- W M Stallard, K-C Wu, N Shi, and M Y Corapcioglu. 1993. "Recirculating Nitrate Treatment Well Hydraulics", AGU Fall 1993 Conference, San Francisco, CA, December 6-10.

- Wilson, J., L. Leach, M. Henson, and J. Jones. 1986. In-situ bioremediation as a ground-water remediation technique. *Ground Water Monitor Review*. p 56.
- Yeh, G. T. 1987. 3DFEWATER: A three-dimensional finite element model of water flow through saturated-unsaturated media. ORNL-6386. Oak Ridge National Laboratory, Oak Ridge, TN.
- Yeh, G. T. 1990. 3DLEWASTE: A three-dimensional finite element model of waste transport through saturated media. Pennsylvania State University Technical Report. The Pennsylvania State University, University Park, PA.

## APPENDIX A—NUMERICAL MODELING RESULTS

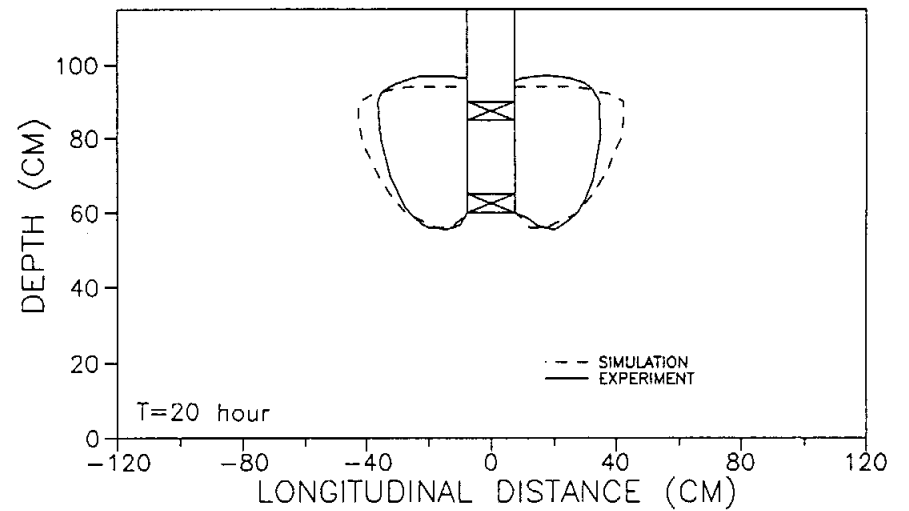
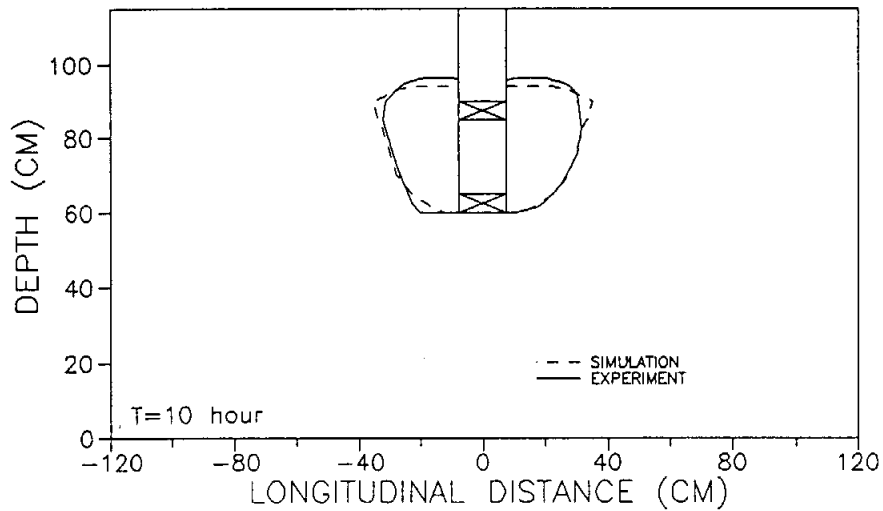
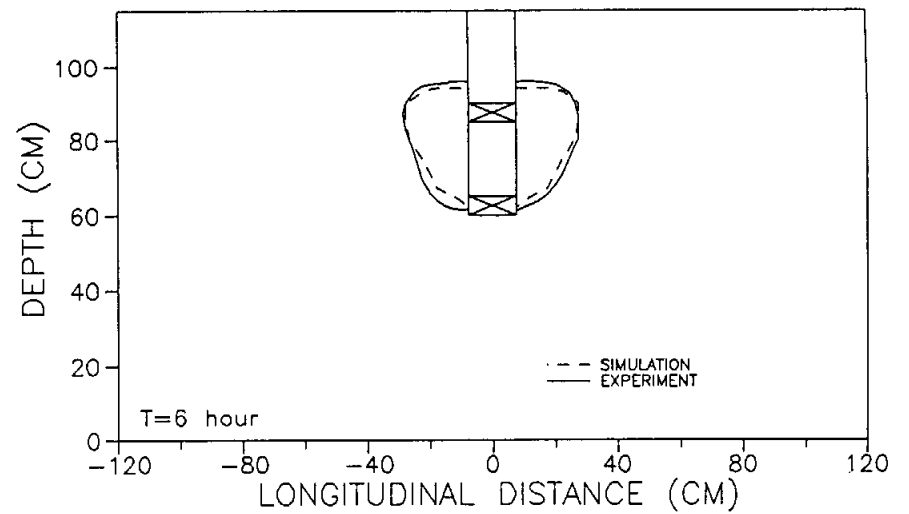
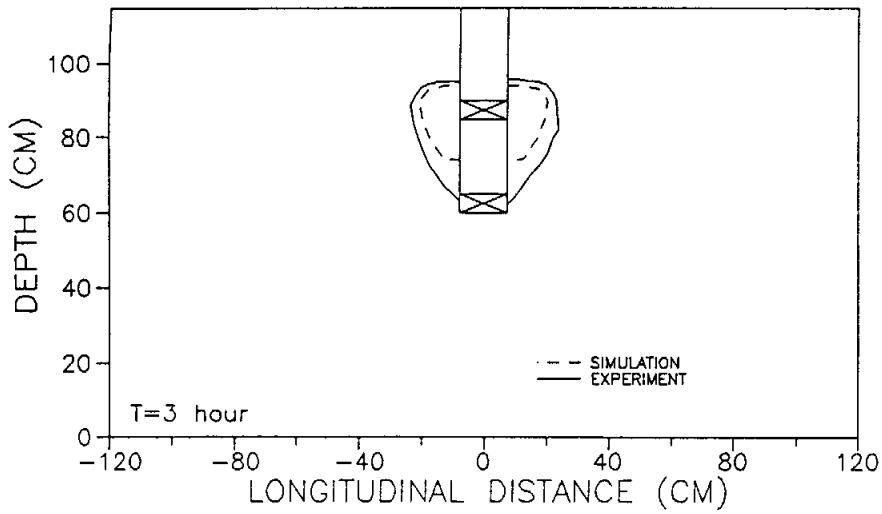


Figure 33. Comparison of numerical and experimental results with no ambient flow velocity, 2.0 m/d internal well velocity, and NaOH added to RGRW with well 1.

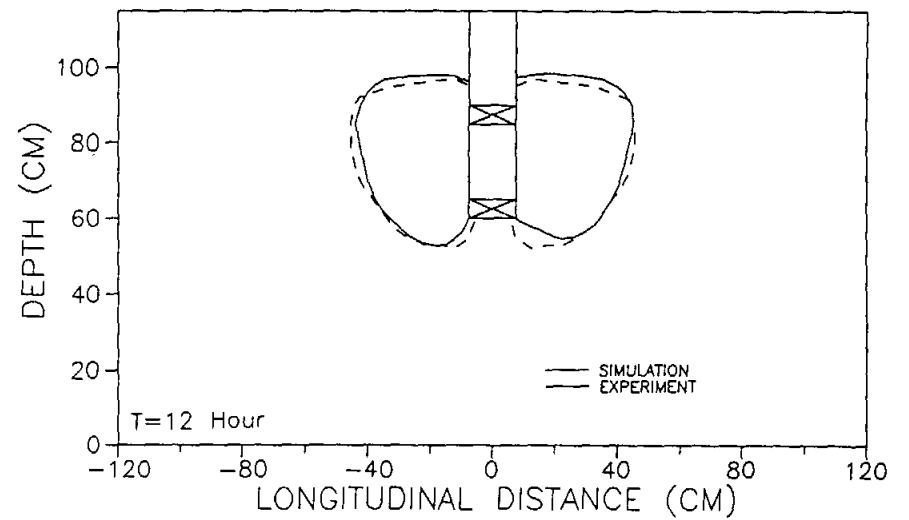
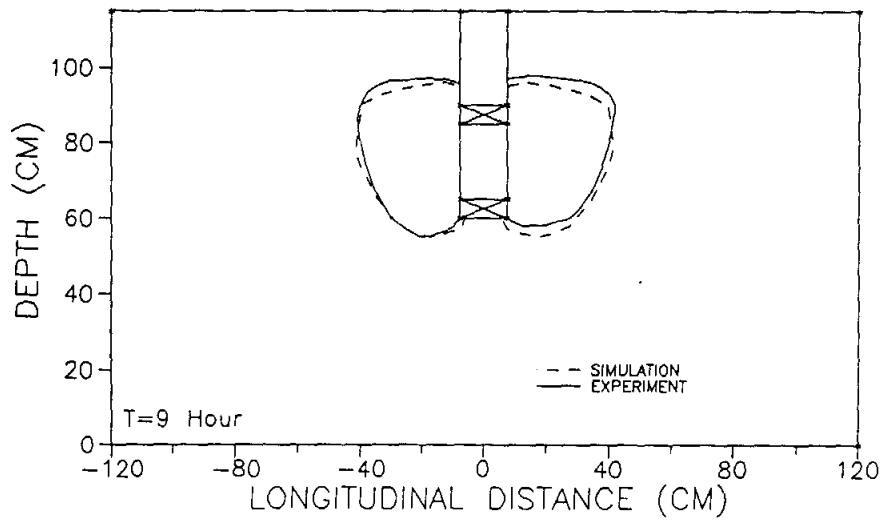
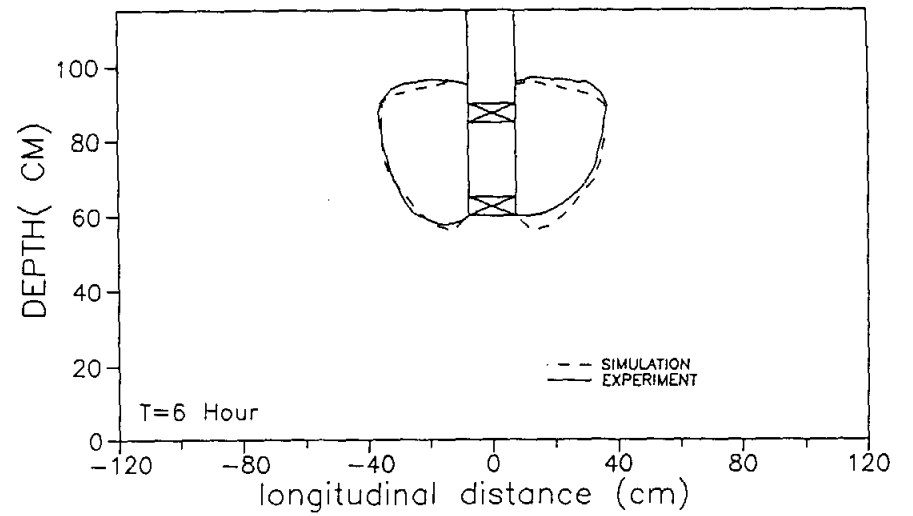
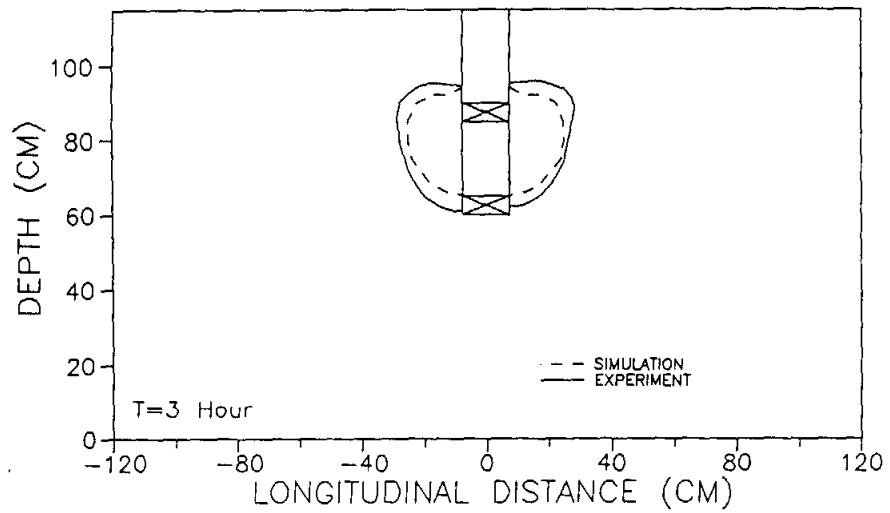


Figure 34. Comparison of numerical and experimental results with no ambient flow velocity, 4.0 m/d internal well velocity, and NaOH added to RGRW with well 1.

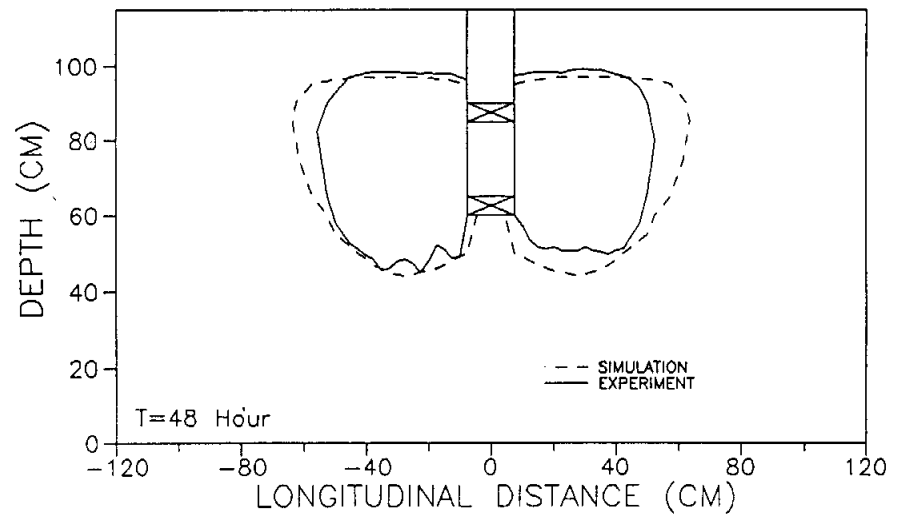
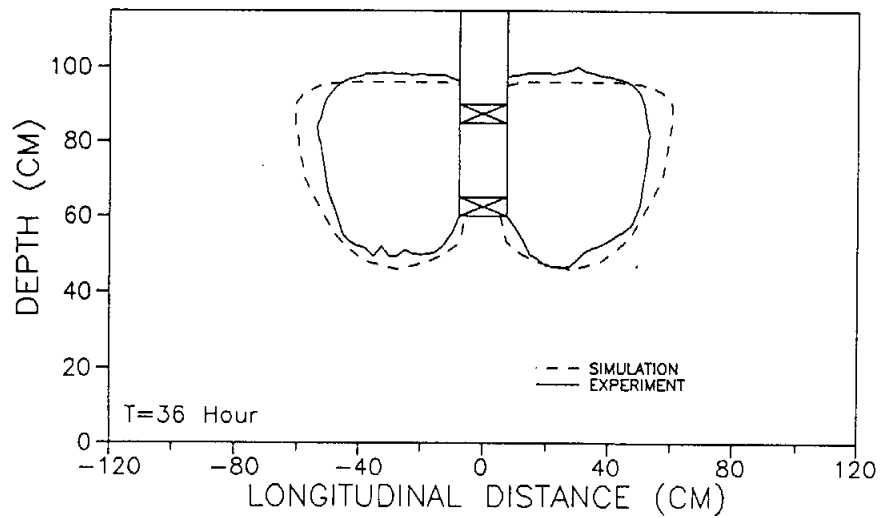
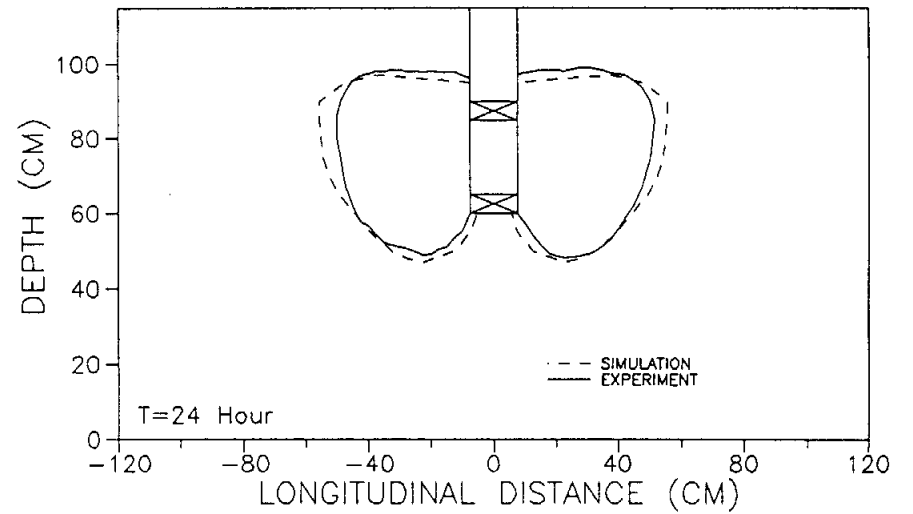
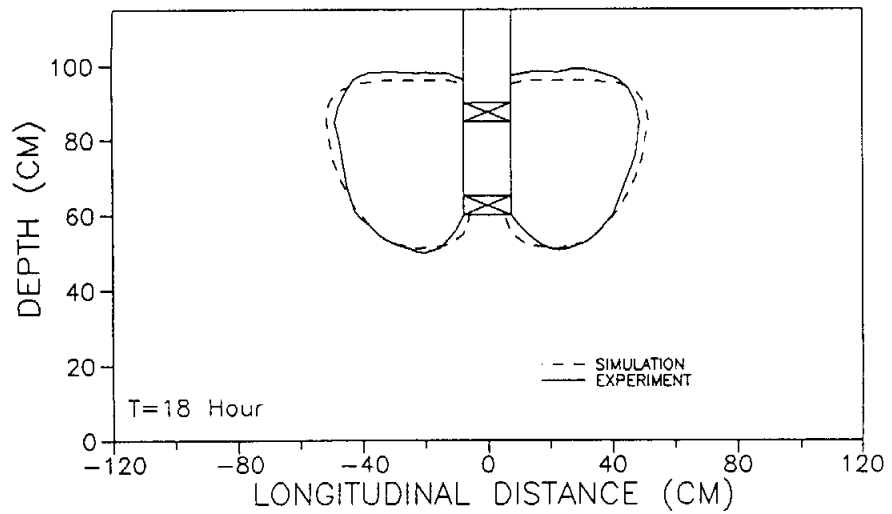


Figure 35. Comparison of numerical and experimental results with no ambient flow velocity, 4.0 m/d internal well velocity, and NaOH added to RGRW with well 1

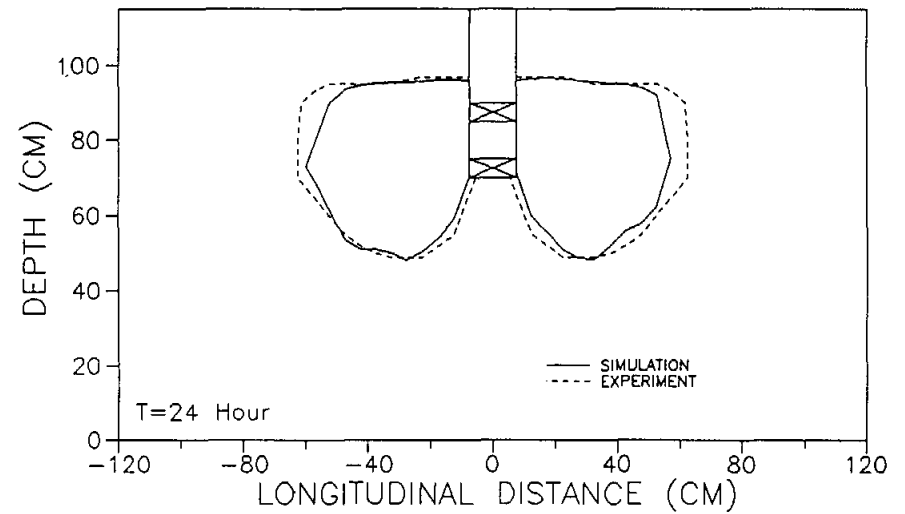
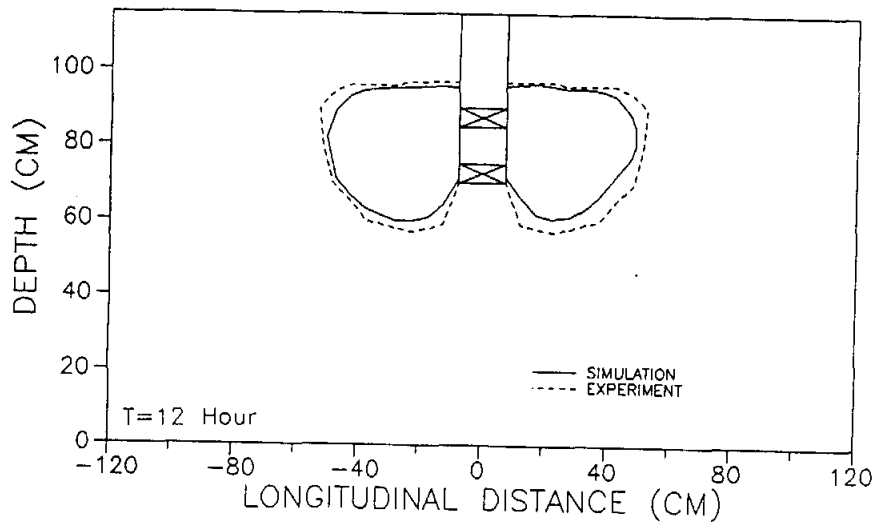
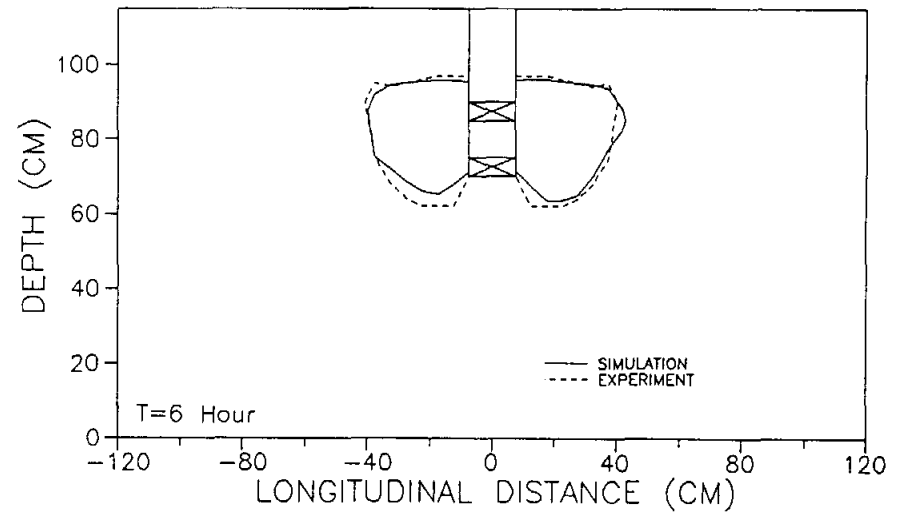
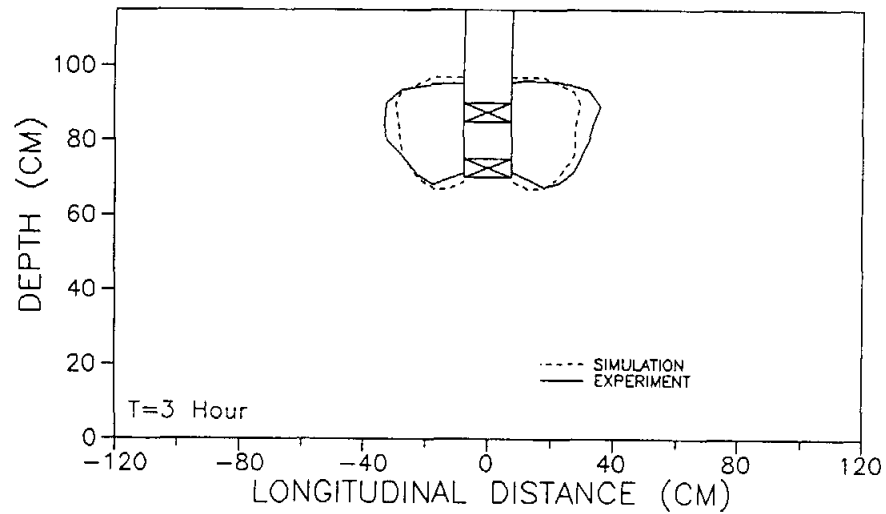


Figure 36. Comparison of numerical and experimental results with no ambient flow velocity, 8.0 m/d internal well velocity, and NaOH added to RGRW with well 2.

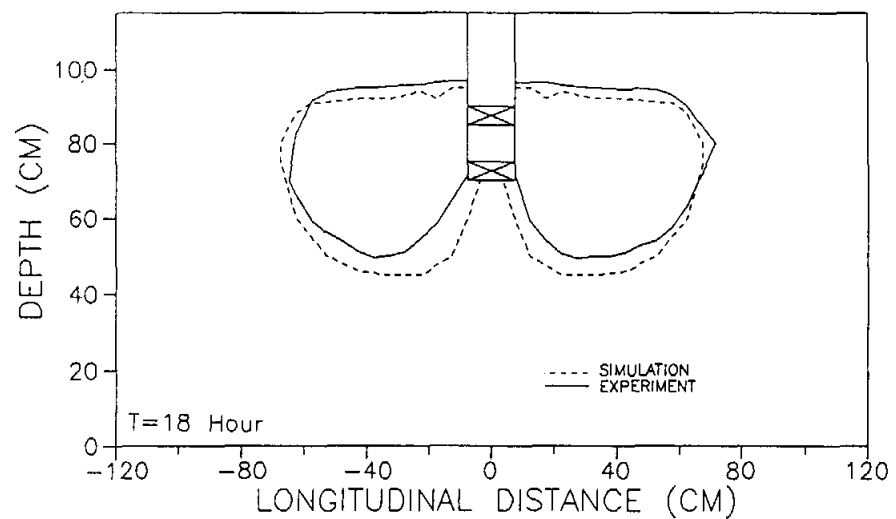
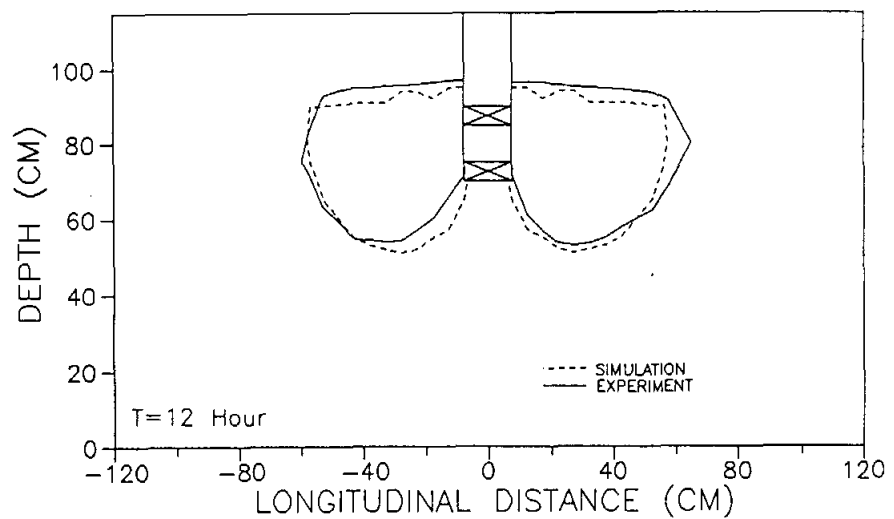
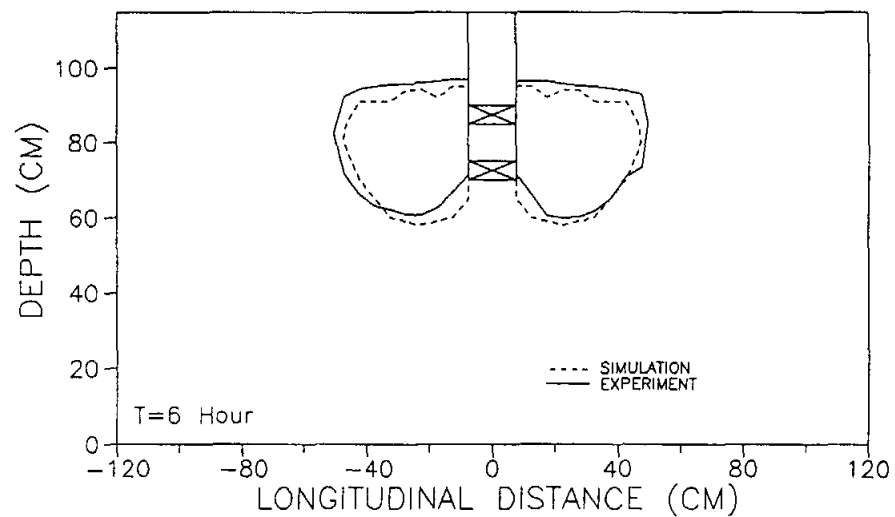
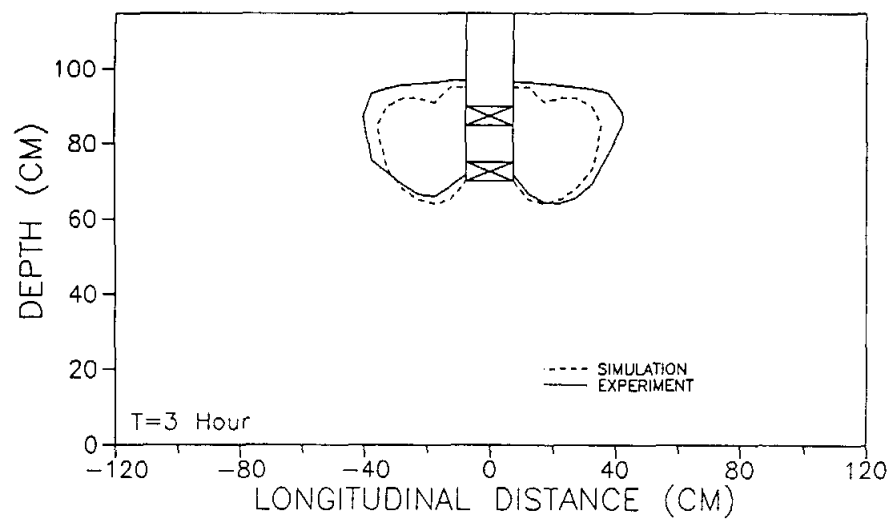


Figure 37. Comparison of numerical and experimental results with no ambient flow velocity, 16.0 m/d internal well velocity, and NaOH added to RGRW with well 2.

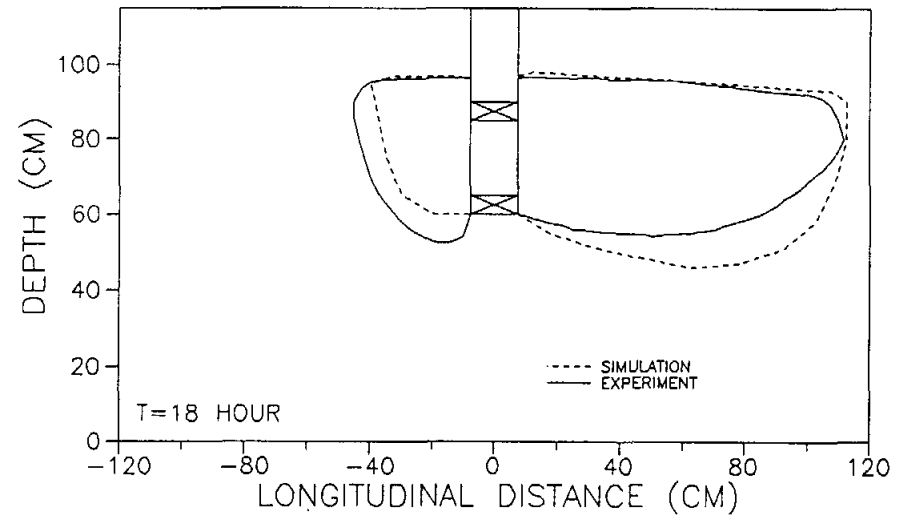
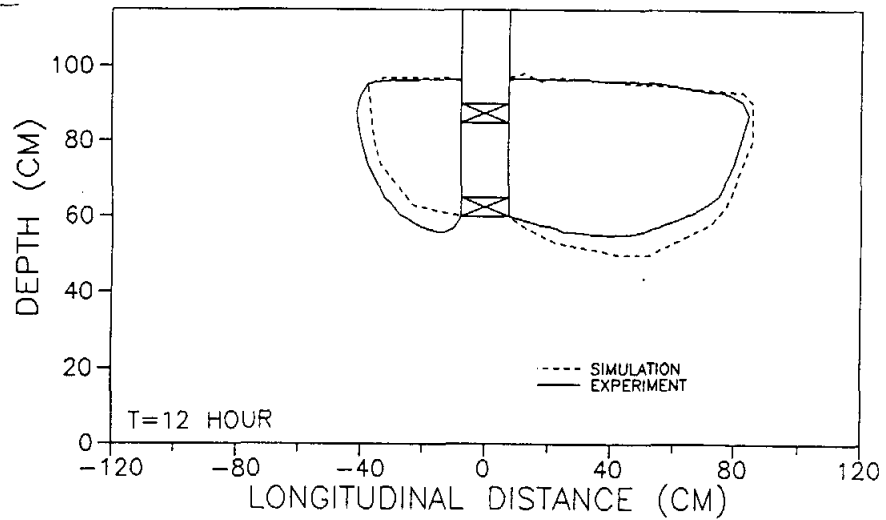
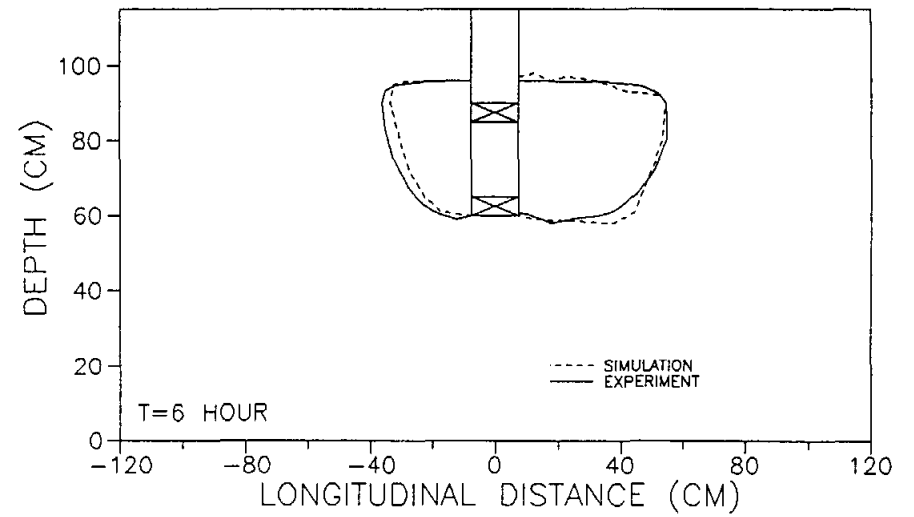
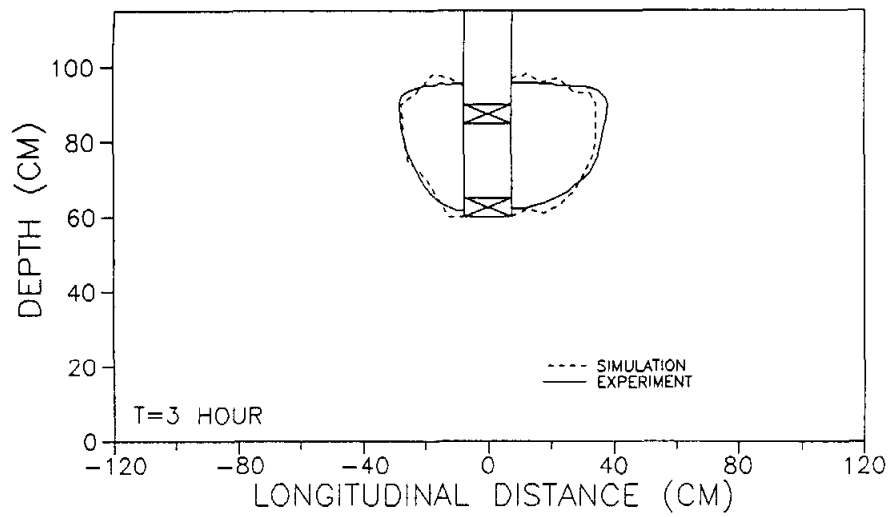


Figure 38. Comparison of numerical and experimental results with 1.0 m/d ambient flow velocity, 4.0 m/d internal well velocity, and NaOH added to RGRW with well 1.

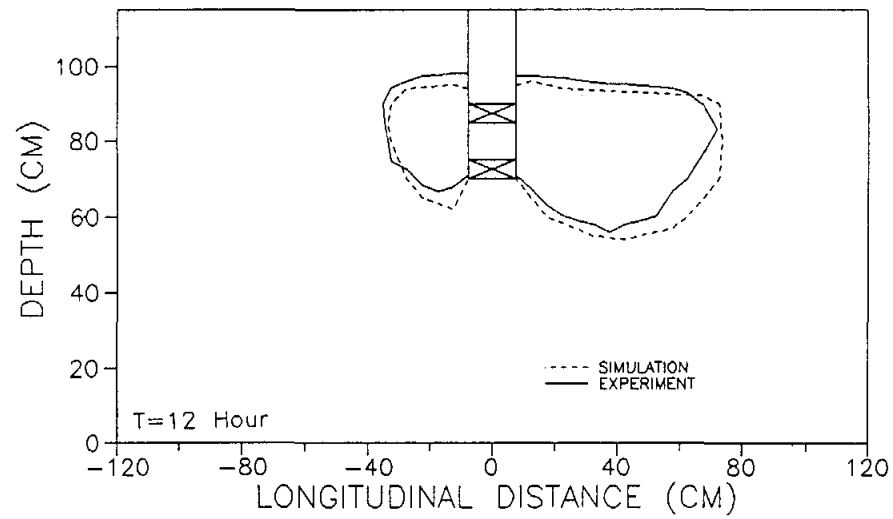
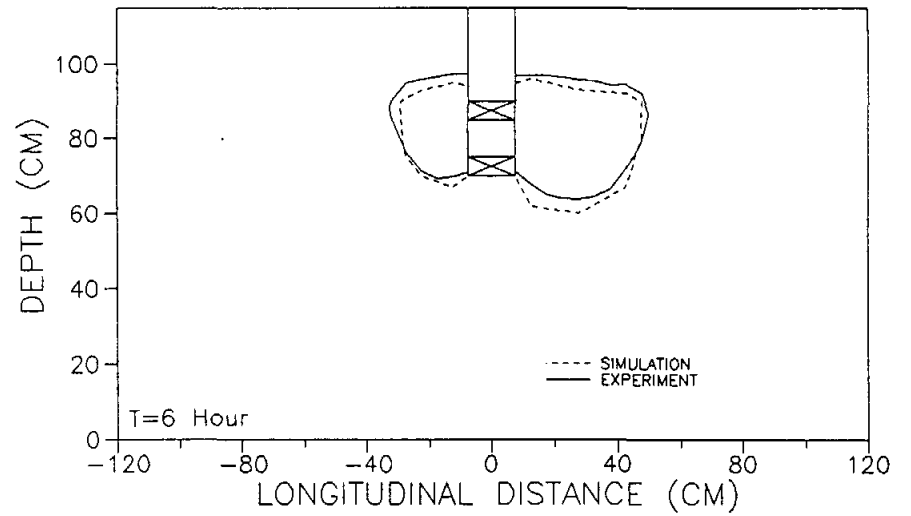
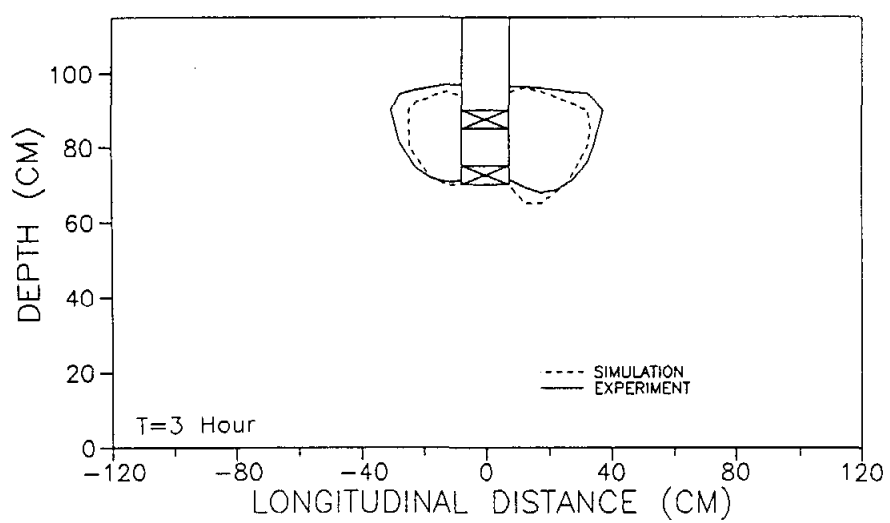


Figure 39. Comparison of numerical and experimental results with 1.0 m/d ambient flow velocity, 8.0 m/d internal well velocity, and NaOH added to RGRW with well 2.

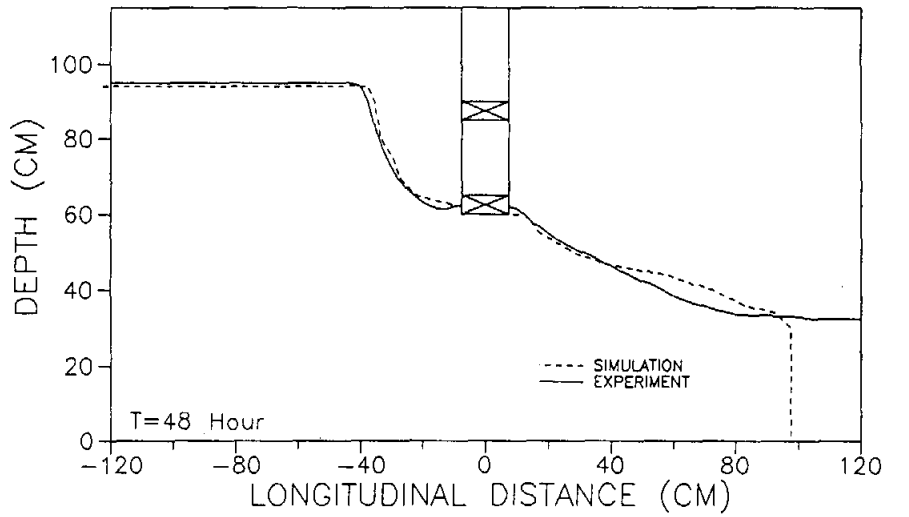
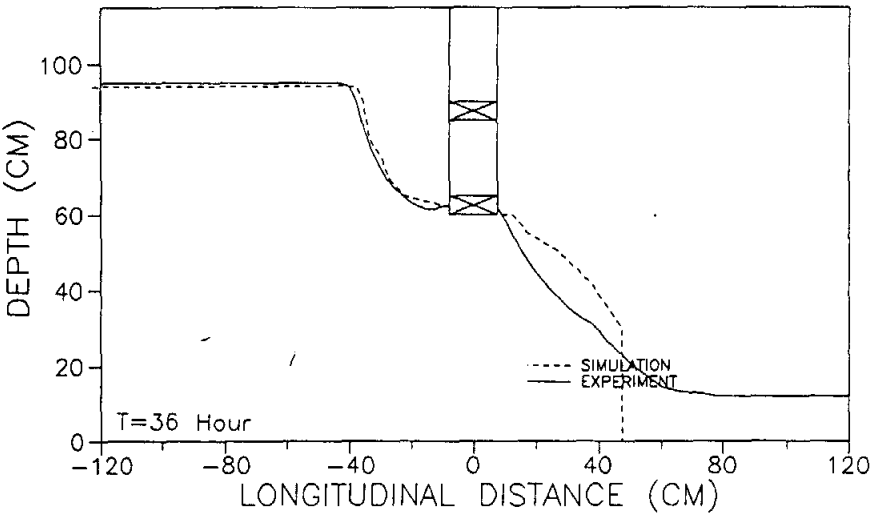
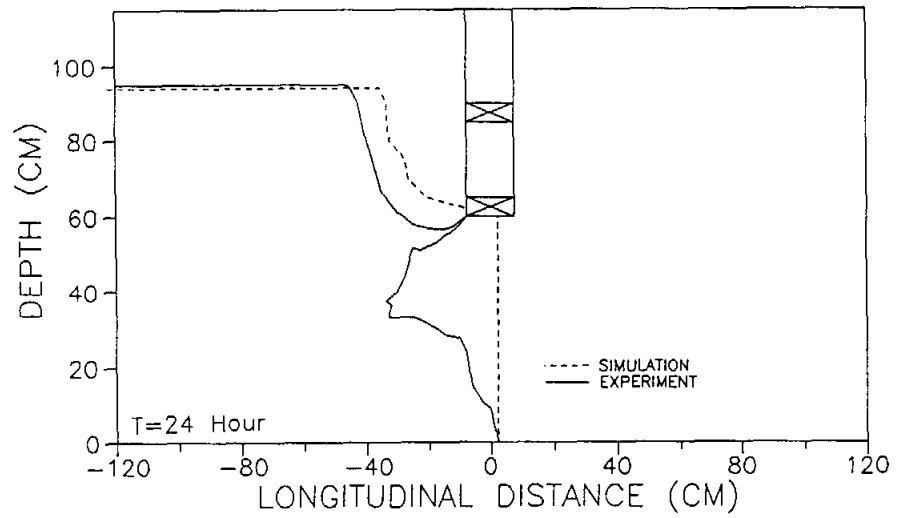
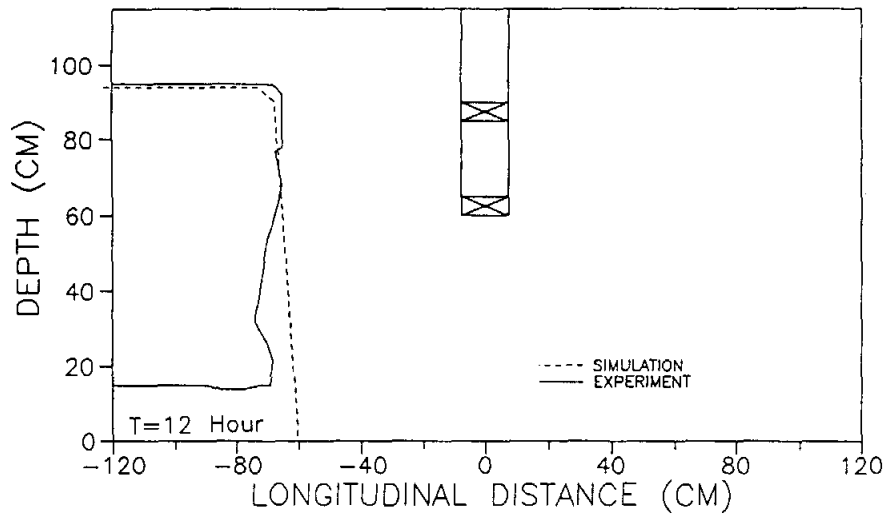


Figure 40. Comparison of numerical and experimental results with 1.0 m/d ambient flow velocity, 8.0 m/d internal well velocity, and NaOH distributed with depth for well 1.

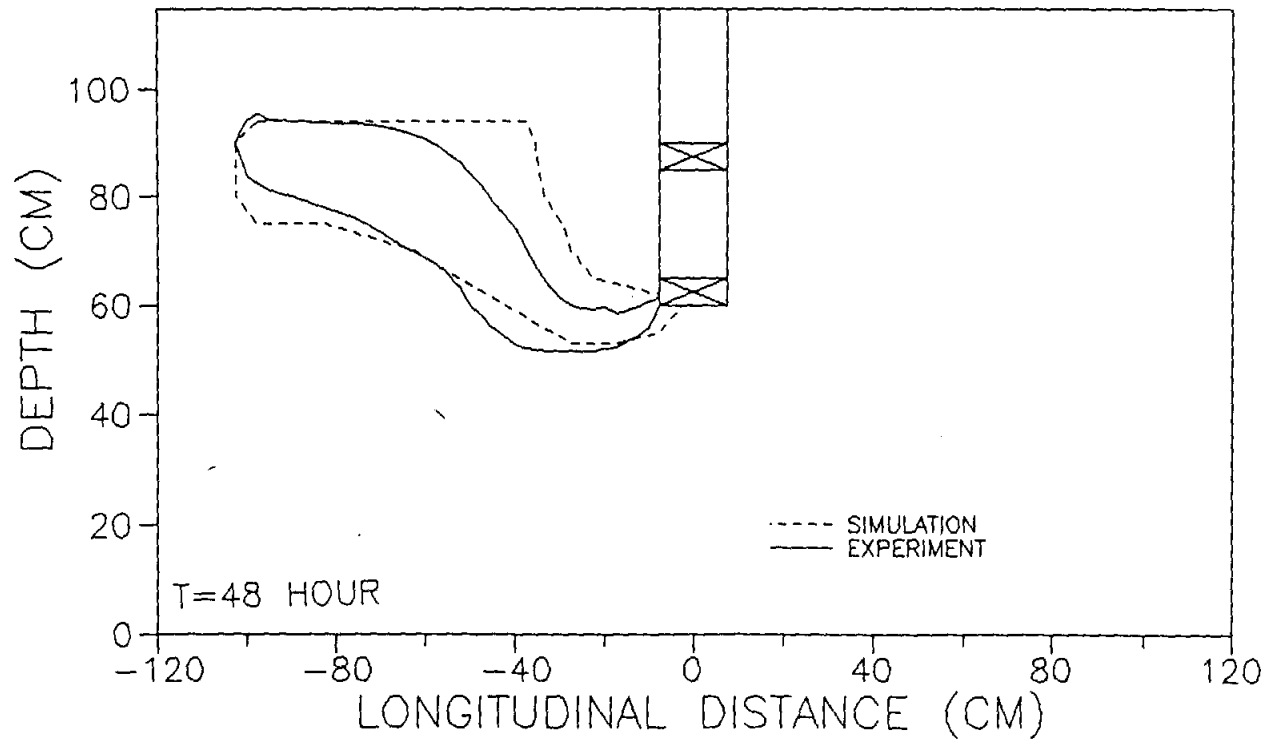


Figure 41. Comparison of numerical and experimental results with 1.0 m/d ambient flow velocity, 4.0 m/d internal well velocity, and NaOH applied at water table with well 1.

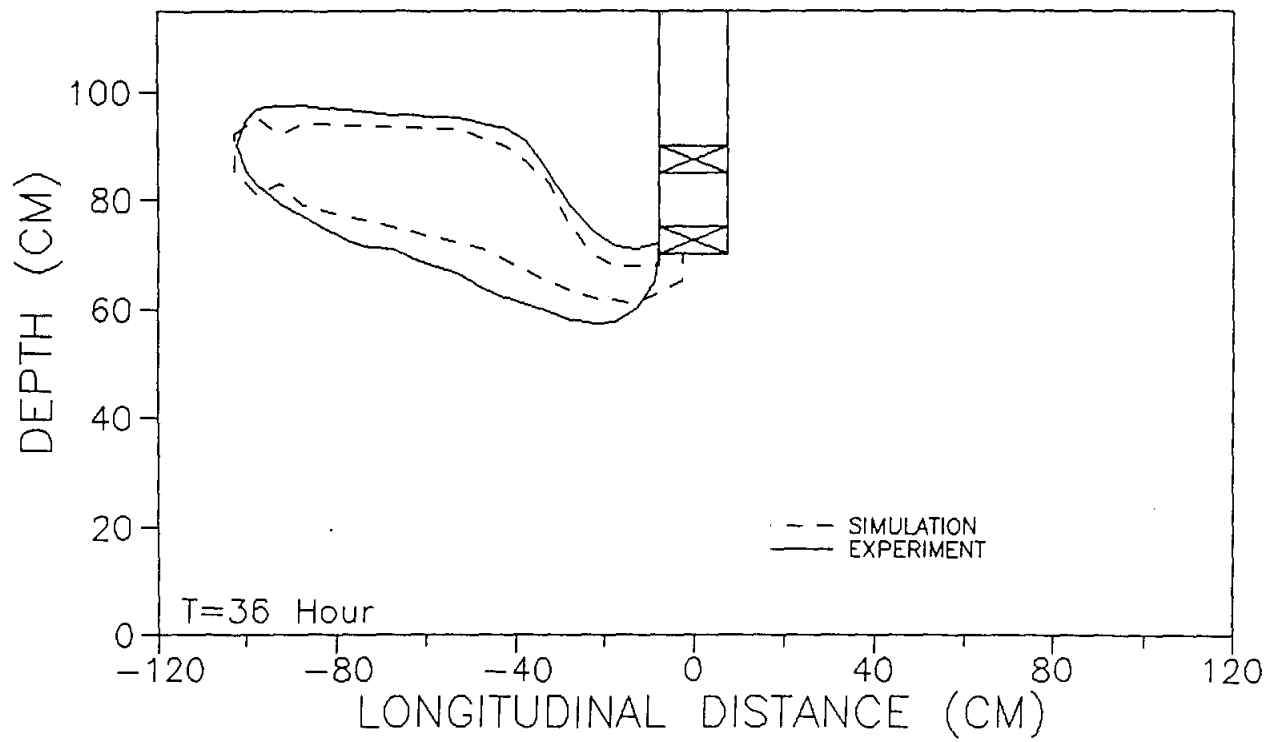


Figure 42. Comparison of numerical and experimental results with 1.0 m/d ambient flow velocity, 8.0 m/d internal well velocity, and NaOH applied at water table with well 2.

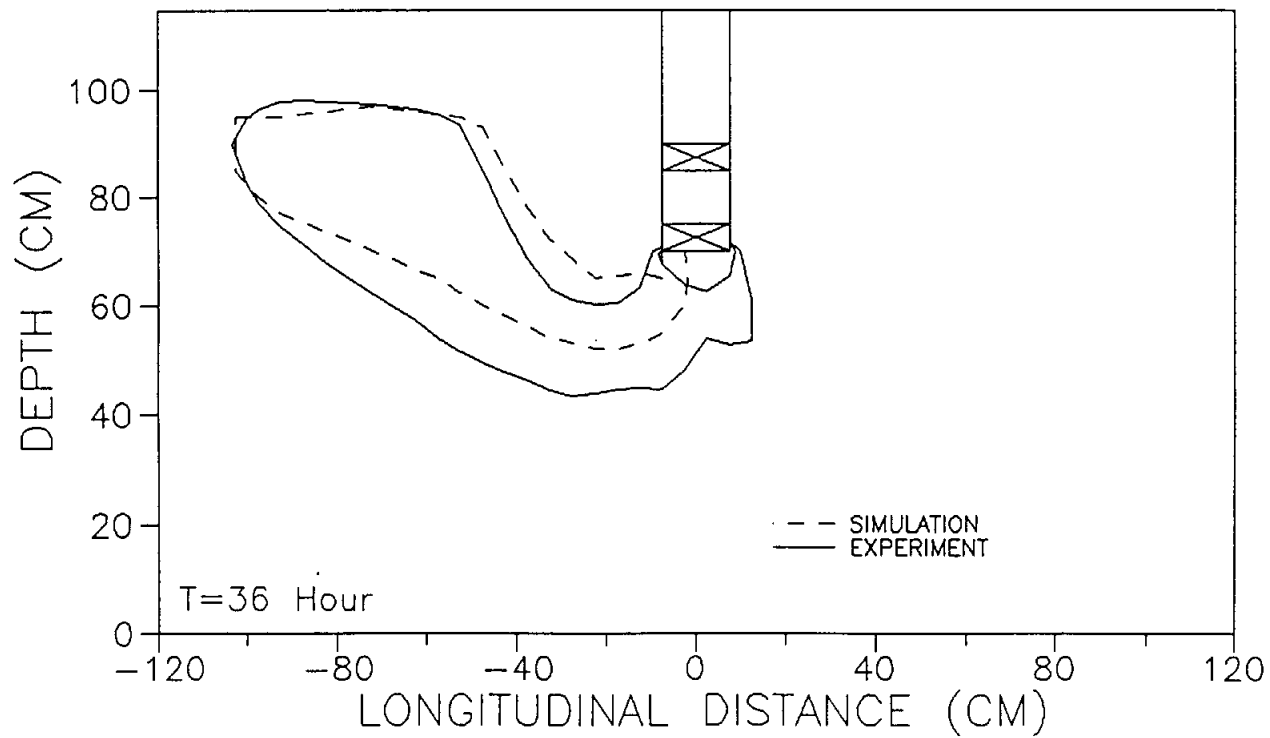


Figure 43. Comparison of numerical and experimental results with 1.0 m/d ambient flow velocity, 16.0 m/d internal well velocity, and NaOH applied at water table with well 2.

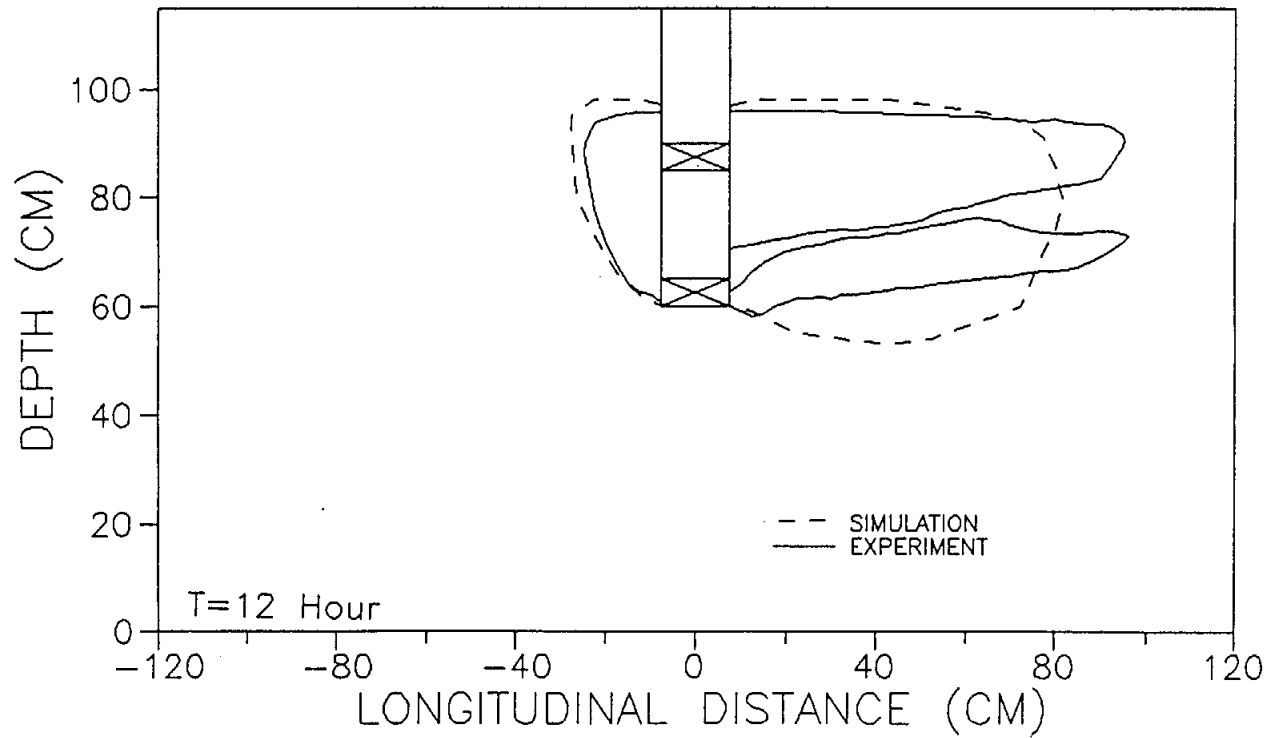


Figure 44. Comparison of numerical and experimental results with 2.0 m/d ambient flow velocity, 2.0 m/d internal well velocity, and NaOH added to RGRW with well 1.